Extramacrochaetae regulates Notch signaling in the *Drosophila* eye through non-apoptotic caspase activity

Sudershana Nair[1,4]
Nicholas E. Baker[1,2,3,5,6]

1. Department of Genetics
Albert Einstein College of Medicine
1300 Morris Park Avenue
Bronx
NY 10461

2. Department of Developmental and Molecular Biology
Albert Einstein College of Medicine
1300 Morris Park Avenue
Bronx
NY 10461

3. Department of Ophthalmology and Visual Sciences
Albert Einstein College of Medicine
1300 Morris Park Avenue
Bronx
NY 10461

4. Present address: Department of Neuroscience and Physiology
NYU School of Medicine
435 East 30th St
New York, NY

5. Present address: Department of Microbiology and Molecular Genetics
University of California, Irvine
2011 Biological Sciences 3
Irvine, CA 92697-2300

6. Author for correspondence: nebaker@uci.edu

Abstract

Many cell fate decisions are determined transcriptionally. Accordingly, some fate specification is prevented by Inhibitor of DNA binding (Id) proteins that interfere with DNA binding by master regulatory transcription factors. We show that the *Drosophila* Id protein Extra macrochaetae (Emc) also affect developmental decisions by regulating caspase activity. Emc, which prevents proneural bHLH transcription factors from specifying neural cell fate, also prevents homodimerization of another bHLH protein, Daughterless (Da), and thereby maintains expression of the *Death-Associated Inhibitor of Apoptosis* (*diap1*) gene. We found that multiple effects of *emc* mutations on cell growth and on eye development were all caused by reduced *Diap1* levels and corresponding activation of caspases. These effects included acceleration of the morphogenetic furrow, failure of R7 photoreceptor cell specification, and delayed differentiation of non-neuronal cone cells. Within *emc* mutant clones, Notch signaling was elevated in the morphogenetic furrow, increasing morphogenetic furrow speed. This was associated with caspase-dependent increase in levels of Delta protein, the transmembrane ligand for Notch. Posterior to the morphogenetic furrow, elevated Delta cis-inhibited Notch signaling that was required for R7 specification and cone cell differentiation. Thus, *emc* mutations reveal the importance of restraining caspase activity even in non-apoptotic cells to prevent abnormal development, in the *Drosophila* eye through effects on Notch signaling.

Introduction

Inhibitor of DNA binding proteins (Id proteins), which are HLH proteins lacking basic DNA-binding sequences, form inactive heterodimers with proneural bHLH proteins, preventing DNA binding and transcriptional regulation of target genes (Benezra et al., 1990; Cabrera et al., 1994; Ellis, 1994; Ellis et al., 1990; Garrell and Modolell, 1990; Norton, 2000). Accordingly, mutations in Id protein genes, of which there are 4 in mammals and one in *Drosophila*, permit enhanced proneural bHLH function, deregulating neurogenesis at many developmental stages and in many tissues (Ling et al., 2014; Oproescu et al., 2021; Roschger and Cabrele, 2017; Wang and Baker, 2015a).

Is this the only mechanism of Id protein function? Not all Id gene mutant phenotypes resemble gain of proneural gene function (Ling et al., 2014; Wang and Baker, 2015a). The sole *Drosophila* Id protein gene *extra macrochaetae* (*emc*) is required for normal growth of imaginal discs (Garcia-Alonso and Garcia-Bellido, 1988). Imaginal discs are larval progenitors of adult tissues and remain proliferated and undifferentiated until late in the final larval instar; no proneural gene is active in these proliferating cells. A second example is that *emc* is required for ovarian follicle cell development (Adam and Montell, 2004), which does not depend on proneural bHLH genes. In *Drosophila* eye development, *emc* is required for the specification of the R7 photoreceptor cells and the non-neuronal cone cells, neither of which depends on any known proneural bHLH gene, and also restrains the rate at which the morphogenetic furrow, a wave of fate specification that traverses across the eye imaginal disc as retinal patterning and differentiation begin (Bhattacharya and Baker, 2009; Brown et al., 1995).

Insights into how Emc acts independently of proneural genes have emerged from several studies. Regarding the proper proliferation of imaginal disc cells (Garcia-Alonso and Garcia-Bellido, 1988), independence of imaginal disc growth from proneural bHLH genes is confirmed by the lack of requirement for *da*, the only E protein in *Drosophila* (Andrade-Zapata and Baonza, 2014; Bhattacharya and Baker, 2011). E proteins are ubiquitously expressed bHLH proteins that are heterodimer partners for proneural bHLH proteins. Proneural bHLH proteins cannot function without Da, so normal growth of *da* mutant cells implies independence from all Da heterodimer partners. It is ectopic Da activity that causes poor growth in *emc* mutant cells, because normal growth is restored in *emc da* double mutant cells (Bhattacharya and Baker, 2011). Elevated Da levels are elevated activate transcription of *expanded* (*ex*), a component of the Salvador-Warts-Hippo (SWH) tumor suppressor pathway to inhibit growth of imaginal disc cells (Wang and Baker, 2015b).

In the course of these studies, we noticed that *ex* mutations affected the number of sensory organ precursor (SOP) cells in the thorax (Wang and Baker, 2015b). This was due to activity of Yorkie (Yki), the transcription factor target of SHW signals, in the *ex* mutant cells. This in turn increased transcription of a direct Yki target gene, *Death-Associated Inhibitor of Apoptosis 1* (*diap1*) (Wang and Baker, 2019). Diap1 is a ubiquitin ligase that prevents accumulation of a processed form of Dronc, an apical caspase in *Drosophila* (Hawkins et al., 2000b; Meier et al., 2000a). Caspases are proteases that drive apoptosis by cleaving cellular substrates. They are expressed as inactive zymogens that are then activated by signals (initiator caspases) or by cleavage by caspases (effector caspases) in a feed-forward process that is

105 expected to kill cells rapidly once a threshold of caspase activity has been crossed (Fuchs and
106 Steller, 2011). Caspases can also mediate non-apoptotic processes. What differentiates apoptotic
107 from non-apoptotic outcomes is uncertain, as the same caspase cascade of initiator and effector
108 caspases seems to be involved (Aram et al., 2017; Baena-Lopez et al., 2018; Colon-Plaza and Su,
109 2022; Kanuka et al., 2005; Kuranaga and Miura, 2007; Nakajima and Kuranaga, 2017; Su,
110 2020). In *ex* mutants, the increased *diap1* transcription does not affect cell death much but causes
111 an increase in *wg* signaling activity (Wang and Baker, 2019). Wg signaling promotes SOP cell
112 determination in the thorax, and it has been shown previously that Wg signaling is antagonized
113 by caspases, through a mechanism that is non-apoptotic but whose direct target is not yet certain
114 (Baker, 1988; Kanuka et al., 2005; Wang and Baker, 2019).

115 Since *emc* mutations elevate *ex* expression (Wang and Baker, 2015b), we wondered
116 whether *emc* also changes Diap1 levels and affects caspase activities. Increased *ex* expression
117 would be expected to reduce transcription of the *diap1* gene and potentially increase caspase
118 activity, the opposite of what occurs in *ex* mutants. Remarkably, we found that caspase activity
119 was responsible for all the aspects of the *emc* phenotype that we tested. This included reduced
120 growth of imaginal disc cells, accelerated morphogenetic furrow progression, and loss of R7 and
121 cone cells fates in the eye. The effects on eye development all reflected caspase-dependent
122 expression of the Notch ligand Delta, which is known to contribute to morphogenetic furrow
123 progression, and R7 and cone cell fate specification. Thus, caspase-dependent non-apoptotic
124 signaling underlies multiple roles of *emc* that are independent of proneural bHLH proteins.

125
126
127 **Materials and Methods**
128
129 **Drosophila Strains**
130
131 The following stocks were employed in this study and were maintained at 25°C unless otherwise
132 stated - *hsflp;;emc^{AP6} FRT80/TM6B, hsflp;;dronc^{i29}FRT80/TM6B, hsflp;;dronc^{i29}emc^{AP6},*
133 *hsflp;;Df(3L)H99/TM3, hsflp;;Df(3L)H99 emc^{AP6}/TM3, Ubi-GFP M(3)67C FRT80, FRT42*
134 *M(2)56F Ubi-GFP, FRT82 M(3)95A Ubi-GFP, hsflp;; Ubi-GFPFRT80, hsflp*; *Su(H)$^{\Delta 47}$FRT40*,
135 *pie^{eB3} FRT40* (Baker et al., 1992), *psn[v1]FRT80/TM6B, Fz3-RFP*;D/TM6B (kind gift from Yu
136 Kimata, University of Cambridge). We obtained genomic Ci construct from Kalderon lab and
137 used BestGene Inc. to target the transgene on the third chromosome and then recombined these
138 flies to generate *hsflp;;ci+M(3)67Calz FRT80/TM6B;ci94/y+spa.*
139
140 **Mosaic Analysis**

141 Mosaic clones were obtained using FLP/FRT mediated mitotic recombination (Golic, 1991; Xu
142 and Rubin, 1993). For non-Minute genotypes, larvae were subjected to heat shock for 30 minutes
143 at 37°C, 60 ± 12 hours after egg laying. For Minute genotypes, heat shock was performed 84 ±
144 12 hours after egg laying for 50 minutes. Larvae were dissected 72 hours after heat shock. All
145 flies were maintained at 25°C unless otherwise stated.

146 **Clonal growth measurements**

Clone and twin-spot areas were measured by tracing in ImageJ. To quantify the growth effects of various genotypes, the sum of clone areas per wing disc was divided by the sum of twin spot areas in the same wing disc. This avoids any subjectivity in identifying individual clones and assigning them to individual twin spots. Clone/Twin-spot ratios were log-transformed to ensure normality before statistical analysis.

Immunohistochemistry and histology

Unless otherwise noted, preparation of eye and wing imaginal discs for immunostaining and confocal imaging were performed as described previously (Baker et al., 2014). Antibodies from Developmental Studies Hybridoma Bank (DSHB): anti-Ptc (mouse, 1:40), anti-Elav (mouse, 1:100), anti-Elav (rat, 1:50, anti-Cut (mouse, 1:50), anti-Delta C594.9B (mouse, 1:2000), anti-βGal (mouse, 1:100), mouse anti-βGal (1:100, DSHB 40-1a) and anti-Ci (rat, 1:10). Other antibodies: anti-phospho-Smad1/5 (rabbit, 1:100, Cell Signaling), anti-DIAP1 (rabbit, 1:50) (gift from Hyun Don Ryoo, NYU), anti-Dcp1 (rabbit, 1:100, Cell Signaling), anti-Sens (guinea pig, a gift from Hugo Bellen used at 1:50), anti-Da (mouse, 1:200), rabbit anti-Emc (1:40), anti-GFP (rat, 1:50 from Nacalai Tesque # GF090R), rabbit anti-GFP (1:500), rabbit anti-ß-Galactosidase (1:100, Cappel), E(spl)bHLH (1:50,mAb323) and guinea pig anti-runt (1:500). Secondary antibodies conjugated with Cy2, Cy3 and Cy5 dyes (1:200) were from Jackson ImmunoResearch Laboratories and Alexa 555 (1:500). Multi-labelling images were sequentially scanned with Leica SP8 confocal microscopes and were projected and processed with ImageJ. All images were assembled into figure format using Adobe Illustrator 2020.

Quantifying immunofluorescence

<u>Anti-DIAP1 and anti-Dl labeling were quantified within clones using the average density measurement in Image J and normalized to control regions in the same tissue. For anti-DIAP1 labeling, in particular, we lack any measurement of any non-specific background labeling that may occur. Differences in Diap1 levels between genotypes may be underestimated if a component of the labeling is non-specific.</u>

Terminal deoxynucleotidyl transferase dUTP nick end labeling (TUNEL) assay

For labeling dead cells with TUNEL assay, ApopTag® Red In Situ Apoptosis Detection Kit (Cat #S7165) was used according to manufacturer's instruction. Briefly, dissected eye discs were fixed for 20 minutes at room temperature followed by three washes with 1X PBS. Then the samples were incubated in equilibration buffer for 1 minute followed by incubation in reaction buffer (TdT enzyme; ratio 7:3) at 37 °C for 1 hour. TdT reaction mix was replaced with stop buffer (diluted 1:34 in dH2O) and incubated for 10 min at room temperature. Samples were washed three times with 1X PBS, 5 min per wash; and incubated with anti-digoxigenin antibody solution (diluted 31:34 in blocking solution) for 30 min at room temperature. The samples were then washed three times in 1X PBS, 5 min per wash. For the subsequent antibody staining, the samples were blocked in PBST (1X PBS + 0.5% Triton-X) for 30 min, and incubated with

primary antibodies in PBST overnight at 4 °C. The samples were next washed with PBST and incubated for 2 h with secondary antibodies in PBST, and then again washed with PBST, followed by PBS wash and samples were mounted in mounting media.

Statistical analysis

Statistical analysis was performed using GraphPad Prism 7. The statistical tests used are described in the figure legends. Statistical significance is shown as follows; n.s., $P > 0.05$; *$P < 0.05$; **$P < 0.01$; ***$P < 0.001$; ****$P < 0.0001$.

Prediction of caspase cleavage sites

Caspase cleavage sites were predicted for Delta using Cascleave 2.0(Wang et al., 2014). Cascleave 2.0 was set to a medium stringency threshold for prediction of cleavage sites.

Results

Caspase activity causes growth defects in *emc* mutants

To determine the contribution of caspases to growth inhibition in *emc* mutant cells, we used the FLP/FRT system (Xu and Rubin, 1993) to generate clones of *emc* mutant cells that were unable to activate caspases normally. We achieved this by homozygously deleting the linked *reaper* (*rpr*), *head involution defective* (*hid*) and *grim* genes using *Df(3L)H99*. Rpr, Hid and Grim proteins promote Diap1 degradation in response to apoptotic stimuli and allow activation of initiator caspases such as *dronc* to start apoptosis (Yoo et al., 2002). By removing all three pro-apoptotic proteins, *Df(3L)H99* affects both apoptotic and non-apoptotic caspase functions in *Drosophila* (Tapadia and Gautam, 2011; White et al., 1994). Thus, clones of *emc Df(3L)H99* mutant cells should be defective for caspase activation. In addition, we also made clones of *emc* mutant cells also mutated for *dronc*, which encodes the main initiator caspase in *Drosophila* that is necessary for most developmental apoptosis (Hawkins et al., 2000a; Meier et al., 2000b; Quinn et al., 2000). Dronc contributes to non-apoptotic caspase functions as well, so *emc dronc* mutant cells should also show reduced non-apoptotic and well as apoptotic caspase functions.

In comparison to neutral clones, which grew equivalently to their twin-spot controls, *emc* mutant clones showed greatly reduced growth in eye or wing imaginal discs, as described previously (Figures 1A-D) (Andrade-Zapata and Baonza, 2014; Bhattacharya and Baker, 2011; Garcia-Alonso and Garcia-Bellido, 1988). By contrast, *emc* mutant clones that were also mutant for *dronc*, or *emc Df(3L)H99* clones that lacked the *rpr*, *grim* and *hid* genes, grew more like their twin spot controls in both eye and wing (Figures 1E-H). Deletion of the *rpr*, *hid* and *grim* genes restored growth indistinguishable from the wild type to *emc* clones, although mutation of *dronc* rescued less completely (see Figure 1N for quantification). Neither homozygosity for *dronc*, nor deletion of *rpr*, *grim* and *hid*, affected growth of otherwise wild type imaginal disc clones (Figure 1I-L).

Previous studies of *emc* phenotypes have often used Minute genetic backgrounds (i.e. heterozygosity for mutations in *Rp* genes) to retard growth and enhance the size of the *emc*

235 mutant clones (Bhattacharya and Baker, 2009). When *emc Df(3L)H99* clones were induced in the
236 *M(3)67C* background, the clones took over almost the entire disc, leaving only a few *M(3)67C*
237 heterozygous cells remaining (Figure 1M). The growth advantage of *emc dronc* clones was not
238 so marked.
239 These results indicate that the growth disadvantage of *emc* mutant imaginal disc clones is
240 mostly attributable to cell death genes. Preventing caspase activation, either by mutating the
241 main initiator caspase, or by preventing Diap1 turnover, partially or completed restored normal
242 growth. Our data did not support a previous suggestion that *dronc* was required for normal wing
243 disc growth (Verghese et al., 2012).
244
245 **Emc regulates furrow progression through non-apoptotic caspase activity**
246
247 *Emc* mutations have multiple effects on the eye imaginal disc, although only a few
248 aspects of retinal differentiation depend on proneural bHLH genes. The proneural gene *atonal* is
249 required, along with *da*, for the specification of R8 photoreceptor precursors in the
250 morphogenetic furrow that initiate each ommatidial cluster in the larval eye disc (Brown et al.,
251 1996; Jarman et al., 1994). Later, during pupal development, proneural genes of the Achaete-
252 Scute gene Complex (AS-C), along with *da*, are required for the specification of the
253 interommatidial bristles (Cadigan et al., 2002). All the other cell types develop independently of
254 proneural bHLH genes, and most of them develop independently of *da* (Brown et al., 1996;
255 Jimenez and Campos-Ortega, 1987).
256 In *emc* mutant clones, retinal differentiation begins precociously, associated with more
257 rapid transit of the morphogenetic furrow across the disc (Figure 2A, B) (Bhattacharya and
258 Baker, 2011, 2012; Brown et al., 1995). By contrast, we found that 75% of the time, the
259 morphogenetic furrow progressed normally through *emc dronc* double mutant clones (Figure
260 2C). Eye discs containing *emc Df(3L)H99* double mutant clones always appeared completely
261 normal (Figure 2D). Both *dronc* and *Df(3L)H99* mutant clones also showed normal furrow
262 progression in the absence of *emc* mutations (Figure 2 Figure Supplement 1A,B).
263 In addition, *emc* mutant clones also exhibit sporadic ectopic differentiation of neurons
264 anterior to the morphogenetic furrow, which do not take photoreceptor cell fate (Figure
265 2A,B).(Bhattacharya and Baker, 2011; Brown et al., 1995). This was likewise absent from *emc*
266 *dronc* and *emc Df(3L)H99* double mutant clones (Figure 2C,D).
267 The overall pattern of retinal differentiation revealed by labeling for Senseless, which is
268 specific for R8 photoreceptor cells in the retina, and Elav, which labels all neuronal
269 photoreceptor cells, appeared so normal in these genotypes that we deemed it necessary to
270 confirm that the supposedly *emc dronc* mutant and *emc Df(3L)H99* mutant clones were indeed
271 mutated for *emc*. This was confirmed by lack of staining by an antibody against Emc protein,
272 similar to plain *emc* mutant clones that did affect the morphogenetic furrow (Figure 2 Figure
273 supplement 1C-E). We also found that *emc dronc* and *emc Df(3L)H99* clones upregulated Da
274 protein expression to a comparable degree to plain *emc* mutant clones (Figure 2 Figure
275 Supplement 1C-E) (Bhattacharya and Baker, 2011). This further confirmed the absence of *emc*
276 function from *emc dronc* mutant and *emc Df(3L)H99* genotypes, and also showed that cell death
277 pathways were not required for the regulation of Da protein levels by *emc*.
278 We have previously concluded that *diap1* transcription is reduced in *emc* mutant clones,
279 and in Da-overexpressing cells, due to Yki inhibition downstream of *ex* (Wang and Baker,
280 2015b). In eye imaginal discs, Diap1 protein was normally present uniformly (Figure 3A).

281 Diap1 protein levels were cell-autonomously reduced in *emc* mutant clones posterior to the
282 morphogenetic furrow, compared to *emc*/+ cells in the same eye discs, and shown and quantified
283 in (Figure 3B, E). A comparable reduction was also seen in *emc Df(3L)H99* clones, compared to
284 *emc*/+ *Df(3L)H99*/+ cells in the same eye discs (Figure 3C,E). There was also no difference in
285 Diap1 levels between *Df(3L)H99* homozygous clones and *Df(3L)H99*/+ cells in the same eye
286 discs (Figure 3D,E). These data suggest *emc* affects Diap1 protein levels, whereas *rpr*, *grim* and
287 *hid* affect Diap1 protein activity. A caveat is that Diap1 levels in mutant clones were not
288 compared directly to wild type cells, none of which were present in the same eye discs, and that
289 *Df(3L)H99* might affect Diap1 protein levels dominantly. Interestingly, we did not detect *emc*-
290 dependent changes in Diap1 levels in wing discs (Figure 3 Figure supplement 1B).
291 To test the role of Diap1 in the eye directly, *diap1* was over-expressed in the posterior
292 eye by transcription under GMR-Gal4 control. This rescued morphogenetic furrow speed to
293 normal in *emc* clones (Figure 3 Figure supplement 2B). We also saw restoration of
294 morphogenetic furrow speed in *emc* clones that expressed Baculovirus P35 under GMR-Gal4
295 control (Figure 3 Figure supplement 2A). Baculovirus P35 encodes a caspase pseudo-substrate
296 that inhibits all *Drosophila* caspases except Dronc (Hawkins et al., 2000b; Hay et al., 1994;
297 Meier et al., 2000b; Xue and Horvitz, 1995). The *emc* clones expressing p35 also lacked cell
298 death (Supplemental Figure 2D). The restoration of morphogenetic furrow speed by Diap1, a
299 *dronc* antagonist, as well as by the caspase inhibitor P35, suggest that the effect of
300 morphogenetic furrow acceleration in *emc* mutant clones is due to the caspase cascade.
301 To test whether reduced Diap1 expression promoted apoptosis and thereby accelerated
302 the morphogenetic furrow, we assessed apoptosis levels by terminal deoxynucleotidyl transferase
303 dUTP nick end labeling (TUNEL) of eye discs containing mutant clones. We found almost no
304 cell death posterior to the furrow in *emc* clones (Figure 3 Figure supplement 2D), and cell death
305 in *emc* clones anterior to the furrow was comparable to controls and less than that of cells
306 surrounding the clones (Figure 3 Figure supplement 2C). Some cell death is expected outside
307 *emc* or control clones, as these cells have the *M* background that is itself associated with an
308 increase in apoptosis(Coelho et al., 2005; Kale et al., 2015; Li and Baker, 2007). Similar to
309 TUNEL, we found no cell death in *emc* clones posterior the furrow with Dcp1 staining (Figure 3
310 Figure supplement 3B).To test whether apoptosis in the eye disc would be sufficient to promote
311 morphogenetic furrow progression, we generated mosaic clones for a *pineapple eye (pie)*
312 mutation. These *pie* mutant cells have an elevated rate of apoptosis in imaginal discs, but not
313 sufficient to prevent *pie* homozygous clones surviving late into larval and even adult life (Shi et
314 al., 2003). The rate of morphogenetic furrow progression was unaffected in eye discs containing
315 *pie* clones (Figure 3 Figure supplement 3A). Because no excess cell death was detected in *emc*
316 clones, and cell death was insufficient to accelerate the morphogenetic furrow in otherwise wild
317 type eye discs, *emc* clones might be affected by a non-apoptotic caspase activity.
318
319 **Wingless and Dpp signaling are unaffected by *emc***
320
321 To understand how caspases could affect the speed of the morphogenetic furrow, we
322 analyzed pathways known to contribute. Hedgehog (Hh) and Decapentaplegic (Dpp) signaling
323 drive this differentiation wave, along with a contribution from Notch signaling (Baonza and
324 Freeman, 2001b; Borod and Heberlein, 1998; Fu and Baker, 2003; Heberlein et al., 1993a; Ma et
325 al., 1993). A negative regulator of morphogenetic furrow progression is Wingless (Wg), which is

326 expressed at the dorsal and ventral eye disc margins (Lee and Treisman, 2002; Maurel-Zaffran
327 and Treisman, 2000).
328 Because we found that *ex* mutations affected thoracic bristle patterning through a
329 caspase-dependent non-apoptotic effect on Wg signaling (Wang and Baker, 2019), we looked
330 first to see whether *emc* mutations reduced Wg signaling in the eye. We used Frizzled-3 RFP
331 (Fz3-RFP) as a reporter (Sato et al., 1999). In control eye discs, the Fz3-RFP recapitulates the
332 pattern of endogenous Wg signaling activity at the wing margins (Figure 4 figure supplement 1)
333 (Treisman and Rubin, 1995). Frizzled-3 RFP expression was not changed in *emc* clones (Figure
334 4A). We then used a mutation in *naked cuticle* (*nkd*), encoding a negative feedback regulator of
335 Wg signaling, to modulate Wg signaling (Chang et al., 2008; Zeng et al., 2000). If the
336 morphogenetic furrow was accelerated in *emc* mutant clones due to reduced Wg signaling, more
337 normal development should occur in *emc nkd* clones. The morphogenetic furrow was still
338 accelerated in *emc nkd* clones, however (Figure 4B). These results provided no evidence that Wg
339 signaling was the relevant *emc* target in the eye.
340 We also examined Dpp signaling, since ectopic Dpp signaling is sufficient to accelerate
341 the morphogenetic furrow (Pignoni and Zipursky, 1997). The pattern of pMad, a readout of Dpp
342 signaling, was identical in *emc* mutant and control clones spanning the morphogenetic furrow
343 (Figure 4C, D). Thus, Dpp signaling did not seem altered by *emc* mutants either.
344
345 **Hedgehog pathway**
346
347 Hedgehog (Hh) signaling is a key mover of the morphogenetic furrow (Heberlein et al.,
348 1993b; Ma et al., 1993; Treisman, 2013). Elevated Hh signaling is sufficient to accelerate the
349 morphogenetic furrow (Heberlein et al., 1995; Ma and Moses, 1995). Notably, it has been
350 suggested previously that *emc* mutations affect the morphogenetic furrow by activating
351 Hedgehog signaling, because *emc* mutant cells accumulate Ci protein (Spratford and Kumar,
352 2013). Full-length Ci protein (Ci155) is targeted to the proteosome by Cul1 for processing into a
353 transcriptional repressor protein Ci75 (Aza-Blanc et al., 1997). By inhibiting this processing, Hh
354 prevents repression of target genes by Ci75 and promotes transcriptional activation downstream
355 of Ci155. Accordingly, Ci155 accumulation is a feature of cells receiving Hh signals (Motzny
356 and Holmgren, 1995).
357 We confirmed that *emc* mutant cells contain higher levels of Ci155, as reported
358 previously (Figure 5A) (Spratford and Kumar, 2013). Ci155 was elevated in *emc dronc* clones
359 (Figure 5B) but reduced to wild-type levels in *emc Df(3L)H99* clones (Figure 5C, Figure 5 figure
360 supplement 1). Thus, Ci155 levels did not correlate perfectly with behavior of the morphogenetic
361 furrow.
362 We noticed that Ci155 levels were elevated in *emc* mutant clones in the posterior,
363 differentiating eye disc, as well as in and ahead of the morphogenetic furrow (Figure 5A). This is
364 significant, because Ci155 is not affected by Hh-dependent Cul1 processing posterior to the
365 morphogenetic furrow (Baker et al., 2009; Ou et al., 2002). Ci155 accumulation posterior to the
366 furrow suggests a Hh-independent mechanism.
367 To test whether Ci155 accumulation in *emc* clones indicates elevated Hh target signaling,
368 we looked at the transmembrane receptor Patched (Ptc) which is a transcriptional target of Hh
369 signaling, acting in a negative feedback loop (Hepker et al., 1997). We saw no changes in Ptc
370 protein levels in either *emc* or *emc Df(3L)H99* clones compared to controls, questioning the
371 notion that Hh signaling was altered by *emc* (Figure 5 figure supplement 2).

372 To test functionally whether Ci155 is responsible for accelerating the furrow in *emc*
373 clones, we generated *emc ci* double mutant clones. To achieve this, a genomic transgene that
374 rescues ci^{94} flies to adulthood (Little et al., 2020), was introduced into chromosome arm 3L
375 where it is linked to the wild type *emc* locus, so that mitotic recombination in the ci^{94} null
376 background leads to *emc ci* double mutant clones. For unknown reasons, *emc ci* double mutant
377 clones were small and difficult to obtain, even in the Minute background. In the *emc ci* double
378 mutant clones we found that spanned the morphogenetic furrow; eye differentiation was still
379 accelerated (Figure 5D). The data, including the unexplained synergistic growth effects, could be
380 consistent with interactions between *emc* and Hh signaling, but they also that *emc* regulates the
381 speed of the morphogenetic furrow through at least one other caspase target besides Ci.
382
383 **Delta expression is a target of caspases**
384
385 The remaining signaling pathway that contributes to morphogenetic furrow movement is
386 Notch. Specifically, only cells where Notch signaling is active are competent to initiate retinal
387 differentiation in response to Dpp (Baonza and Freeman, 2001a; Fu and Baker, 2003).
388 Accordingly, ectopic expression of Delta, the transmembrane ligand for Notch, is sufficient to
389 accelerate retinal differentiation anterior to the morphogenetic furrow by expanding the effective
390 range of Dpp signaling (Baonza and Freeman, 2001a; Li and Baker, 2001).
391 To test whether *emc* restrains Notch, we examined the bHLH proteins of the E(spl)-C,
392 widely characterized targets of the Notch pathway (Bray, 2006). We used mAb323 to detect up
393 to five E(spl) bHLH proteins with Notch-dependent expression (Jennings et al., 1994). E(spl)
394 protein expression, and hence Notch signaling, was higher in the morphogenetic furrow in *emc*
395 clones than in wild type cells (Figure 6A). By contrast, E(spl) protein expression was normal in
396 *emc dronc* clones (Figure 6B).
397 To test whether elevated Notch signaling was required to accelerate the morphogenetic
398 furrow in *emc* mutants, we examined *emc psn* double mutant clones. Presenilin (Psn) is the
399 enzymatic component of γ-secretase that releases the intracellular domain of Notch during active
400 Notch signaling, and the *psn* gene is linked to *emc*. Loss of *psn* function leads to a Notch loss of
401 function phenotype (Struhl and Greenwald, 1999; Ye et al., 1999). Accordingly, *psn* clones lead
402 to a neurogenic phenotype in the eye, without affecting the progression of the morphogenetic
403 furrow (Figure 6C) (Li and Baker, 2001). The position of the morphogenetic furrow was also not
404 affected in *emc psn* clones (Figure 6D). Thus, the furrow was not accelerated in *emc* mutant
405 clones also defective for Notch signaling.
406 These two results together indicated that *emc* mutants promoted Notch signaling in the
407 morphogenetic furrow, acting through caspase signaling on a step prior to γ-secretase cleavage of
408 the intracellular domain of Notch. Accordingly, we decided to check Delta (Dl) protein levels.
409 We found that Dl protein levels were significantly and consistently elevated cell-autonomously
410 throughout *emc* clones, both posterior and anterior to the furrow (Figure 7B,E). Importantly, this
411 includes the region just ahead of the morphogenetic furrow that lacks Delta expression in normal
412 development(Baker and Yu, 1998; Parks et al., 1995) (Figure 7B). By contrast, levels of Dl
413 protein *emc Df(3L)H99* clones were similar to those of wild type controls (Figure 7A,D,E).
414 Levels in *emc dronc* clones were also similar to wild type on average, although some clones
415 seemed to show an increase, smaller than in *emc* clones (Figure 7A,C,E). This indicated that Dl
416 protein is a target of caspases, directly or indirectly. The Delta protein sequence contains
417 multiple predicted caspase target sites, as do many proteins (Wang et al., 2014). Only one

418 candidate site lies in the intracellular domain, where it would potentially be accessible to
419 caspases (Figure 7 supplement 1). Truncation of the Dl intracellular domain is usually associated
420 with loss of Dl function, not stabilization and enhanced function, however (Daskalaki et al.,
421 2011).
422 Because Dl activates Notch signaling cell non-autonomously, we wondered whether the
423 effect of *emc* mutant clones was cell-autonomous. We note that, in all the experiments reported
424 here, and in all the previous studies of *emc* mutant clones affecting morphogenetic furrow
425 movement, the morphogenetic furrow is maintained as a continuous groove across the eye disc
426 (Bhattacharya and Baker, 2011, 2012; Brown et al., 1995; Spratford and Kumar, 2013). That is,
427 the advanced front of retinal differentiation within *emc* clones is always smoothly continuous
428 with the normal morphogenetic furrow outside the clones, implying a progressive gradual
429 increase in morphogenetic furrow speed near the lateral edges of *emc* mutant clones (eg Figures
430 2B, 4B, 4D, 5A, 6A). Clones of *Su(H)* null mutants, which act cell-autonomously, provide a
431 contrasting example. Complete loss of *Su(H)* accelerates the morphogenetic furrow due to loss of
432 default Su(H) repression of Notch targets(Li and Baker, 2001). The boundaries of *Su(H)* null
433 clones exhibit a clear discontinuity between the rates of differentiation within and outside the
434 clones (Figure 6E). This difference between *Su(H)* and *emc* mutant clones is consistent with the
435 idea that *emc* affects morphogenetic furrow progression differently from *Su(H)*.
436
437 **Specific ommatidial cell fates are regulated by caspases in *emc* mutants**
438
439 Because the general pattern of neurogenesis revealed by pan-neuronal anti-Elav staining
440 appeared so normal in *emc dronc* and *emc Df(3L)H99* clones (Figure 2C,D), we examined
441 whether effects of *emc* on particular retinal cell fates was caspase dependent. Emc is also
442 required for R7 differentiation and for timely onset of cone cell differentiation (Bhattacharya and
443 Baker, 2009), two cell fate decisions that also depend on Notch signaling (Cooper and Bray,
444 2000; Flores et al., 2000; Tomlinson and Struhl, 2001; Treisman, 2013). These cell fates are
445 normally independent of *da*, but like imaginal disc cell growth and morphogenetic furrow
446 progression, ectopic *da* activity perturbs them in *emc* mutants (Brown et al., 1996; Reddy et al.,
447 2024).
448 Clones of *emc* mutant cells lack R7 photoreceptor cells (Figure 8A,B) (Bhattacharya and
449 Baker, 2009). R7 differentiation was restored to 90% of ommatidia in *emc Df(3L)H99* clones
450 (Figure 8C). As shown before, *emc* mutant clones delayed cone cell differentiation by 2-3
451 columns (corresponding to a delay of 3-6 h) (Bhattacharya and Baker, 2009)(Figure 8D,E). We
452 found no delay in cone cell differentiation in most *emc Df(3L)H99* clones (Figure 8F). These
453 results indicated that caspase activity contributes to the R7 and cone cell differentiation defects
454 that are also characteristic of *emc* mutants.
455
456 **Discussion**
457
458 The Inhibitor of DNA binding (Id) proteins are important regulators of differentiation (Ling et
459 al., 2014; Massari and Murre, 2000; Roschger and Cabrele, 2017; Singh et al., 2022; Wang and
460 Baker, 2015a). They are well known to antagonize proneural basic helix-loop-helix (bHLH)
461 proteins (Benezra et al., 1990; Cabrera et al., 1994; Ellis, 1994; Ellis et al., 1990; Garrell and
462 Modolell, 1990; Norton, 2000). It has been uncertain whether this is their only function, as in

463 *Drosophila* it is clear that *emc* mutations affect processes that are independent of proneural
464 genes.
465
466 One other known effect of *emc* is that it restrains the *Drosophila* E protein Da. Da is expressed
467 ubiquitously and is the obligate heterodimer partner of proneural bHLH proteins in neurogenesis.
468 In undifferentiated progenitor cells, most or all Da is thought to be sequestered in inactive
469 heterodimers with Emc (Li and Baker, 2018). In *emc* mutant cells, Da levels rise and become
470 functional, potentially as homodimers(Bhattacharya and Baker, 2011). Multiple aspects of *emc*
471 mutants, including poor growth, speed of morphogenetic furrow progression, and R7
472 photoreceptor and cone cells fates, depend on this ectopic *da* activity (Bhattacharya and Baker,
473 2011; Reddy et al., 2024).
474
475 It was noticed, in the context of imaginal disc cell growth, that *emc* mutant cells experience *da*-
476 dependent over-expression of the *ex* gene (Wang and Baker, 2015b, 2018). Although most of the
477 studies on *ex* has focused on its role in growth control through the SWH pathway, *ex* was shown
478 to influence patterning through Yki-dependent transcription of *diap1*, an important regulator of
479 cell death pathways. This was in the developing thorax, where *ex* mutations affect bristle
480 patterning through *diap1* and a non-apoptotic effect of caspases on Wg signaling (Wang and
481 Baker, 2019). This observation led us to explore whether aspects of the *emc* phenotype could
482 reflect reduced *diap1* expression and elevated caspase activity.
483
484 Remarkably, we found that all four features of the *emc* phenotype we examined depended on the
485 caspase-mediated cell death pathway. The normal growth of imaginal disc cells, normal speed of
486 the morphogenetic furrow, specification of R7 photoreceptor cells, and timing of non-neuronal
487 cone cell development were all restored when caspase activation was prevented, which was
488 achieved by inactivating the initiator caspase Dronc, deleting the proapoptotic *rpr*, *grim*, and *hid*
489 genes, over-expressing *diap1*, or over-expressing baculovirus p35. These appeared to be non-
490 apoptotic effects because no elevation in apoptosis was apparent in *emc* mutant cells, because
491 generating apoptosis by another means did not mimic the effects, and because the effects were
492 mediated by elevate Dl protein expression in cells that were not apoptotic. They appeared to be
493 effects of caspase activity because they depended in part on *dronc*, an initiator caspase that
494 cleaves and activates effector caspases, because they were suppressed by baculovirus p35, a
495 caspase inhibitor that is a caspase pseudo-substrate, and because they were suppressed by Diap1,
496 a ubiquitin ligase that targets caspases for degradation. The effects may depend on the full
497 caspase cascade because sensitivity to p35 indicates that caspases other than Dronc are
498 necessary, and because mutating dronc alone gave lesser degrees of rescue than deleting *rpr*,
499 *grim*, and *hid*. This is consistent with many other studies that describe the pathways for
500 apoptotic and non-apoptotic caspase functions as similar (Aram et al., 2017; Baena-Lopez et al.,
501 2018; Colon-Plaza and Su, 2022; Kanuka et al., 2005; Kuranaga and Miura, 2007; Nakajima and
502 Kuranaga, 2017; Su, 2020).
503
504 Whereas non-apoptotic caspase activity promotes Wg signaling during specification of thoracic
505 bristles (Kanuka et al., 2005), in the *Drosophila* eye the non-apoptotic caspase target was Notch
506 signaling, due to elevated Delta protein levels. We do not know whether Delta is the direct
507 caspase target. Dl protein levels could also be elevated through other mechanisms, for example
508 through elevated *Dl* gene transcription, or proteins that affect Dl protein stability.

Notably, *emc* mutations accelerate the morphogenetic furrow by enhancing Notch signaling, potentially non-autonomously, but inhibit R7 and cone cell differentiation through cell-autonomously reduced N signaling (Bhattacharya and Baker, 2009; Reddy et al., 2024). These contrasts may be explained through the dual functions of the Notch ligand Delta in trans-activation and in cis-inhibition (Bray, 2016; Jacobsen et al., 1998; Li and Baker, 2004; Micchelli et al., 1997). The eye disc region ahead of the morphogenetic furrow lacks Delta expression (Baker and Yu, 1998; Parks et al., 1995). Ectopic Dl expression here is sufficient to activate N non-autonomously and drive morphogenetic furrow progression (Baonza and Freeman, 2001a; Li and Baker, 2001). Within the R7 equivalence group, Delta is expressed early in R1 and R6 photoreceptor precursors, protecting them from N activation through cis-inhibition, and establishing the distinction between R1,6 and R7 precursor cells (Miller et al., 2009). Ectopic Dl expression posterior to the morphogenetic furrow has cis-inhibitory effect. Elevated Dl levels within *emc* mutant clones may render potential R7 and cone cell precursors cell-autonomously resistant to N activation, as normally seen in R1/6 precursor cells.

A previous study suggested that *emc* mutations might affect Hh signaling (Spratford and Kumar, 2013). Our data point much more clearly to an effect on Notch signaling. Although the Hh target Ci155 accumulates in *emc* mutant cells, increased Hh signaling is not the only possible cause. Ci155 is cytoplasmic, and thought to be only a precursor for a labile nuclear activator molecule (Ohlmeyer and Kalderon, 1998). Preventing activation and nuclear translocation of Ci155 by mutating the kinase *fused* also leads to Ci155 accumulation, but inactivates Hh signaling, showing that Ci155 levels and Hh activity can be separated. Presumably Ci155 accumulates in *fu* mutants because it is more stable than its activated derivative (Ohlmeyer and Kalderon, 1998). Significantly, *emc* mutant cells have been reported to over-express the *fused* antagonist *su(fu)*, providing a potential alternative explanation of Ci155 accumulation in *emc* mutant cells (Spratford and Kumar, 2013). Analyzing *emc ci* double mutant cells suggested that *ci* was not essential to accelerate the morphogenetic furrow in *emc* mutant clones.

Here, we show that multiple effects of *emc* mutations that occur independently of proneural bHLH genes, due to the loss of restraint on *da* function in *emc* mutant cells, are caused by caspase-dependent non-apoptotic processes that result from reduced expression of Diap1 protein. Caspase-dependent non-apoptotic processes have previously been shown to affect Wg activity in the developing notum, although the direct target remains to be identified. Here we show that in eye development, Notch signaling is the target. Expression of Dl protein is increased in a caspase-dependent manner, which leads either to Notch activation or to Notch inhibition, depending on whether Delta acts through trans-activation or cis-inhibition. Our results show that, in addition to contributing to normal development, non-apoptotic caspase activities contribute to mutant phenotypes. In the *Drosophila* eye, multiple aspects of the *emc* phenotype result from caspase-dependent changes in Notch signaling, one of the major cell-cell signaling pathways that contributes to many, many cell fate decisions, and other, unidentified caspase-dependent events affect the growth of *emc* mutant cells in undifferentiated imaginal discs.

Acknowledgements

We thank Y. Kimata, D. Kalderon, H. Bellen, H.D Ryoo and Developmental Studies Hybridoma Bank for antibodies and Drosophila strains, and Tao Wang for statistical advice. We thank C. Khan, A. Kumar, J. Secombe, and A. Jenny for comments on the manuscript. Confocal microscopy was performed at the Analytical Imaging Facility, Albert Einstein College of Medicine. The Leica SP8 microscope was acquired through NIH SIG 1S10 OD023591. Supported by grants from the NIH (GM047892 and EY028990).

579 **Figure Legends**
580

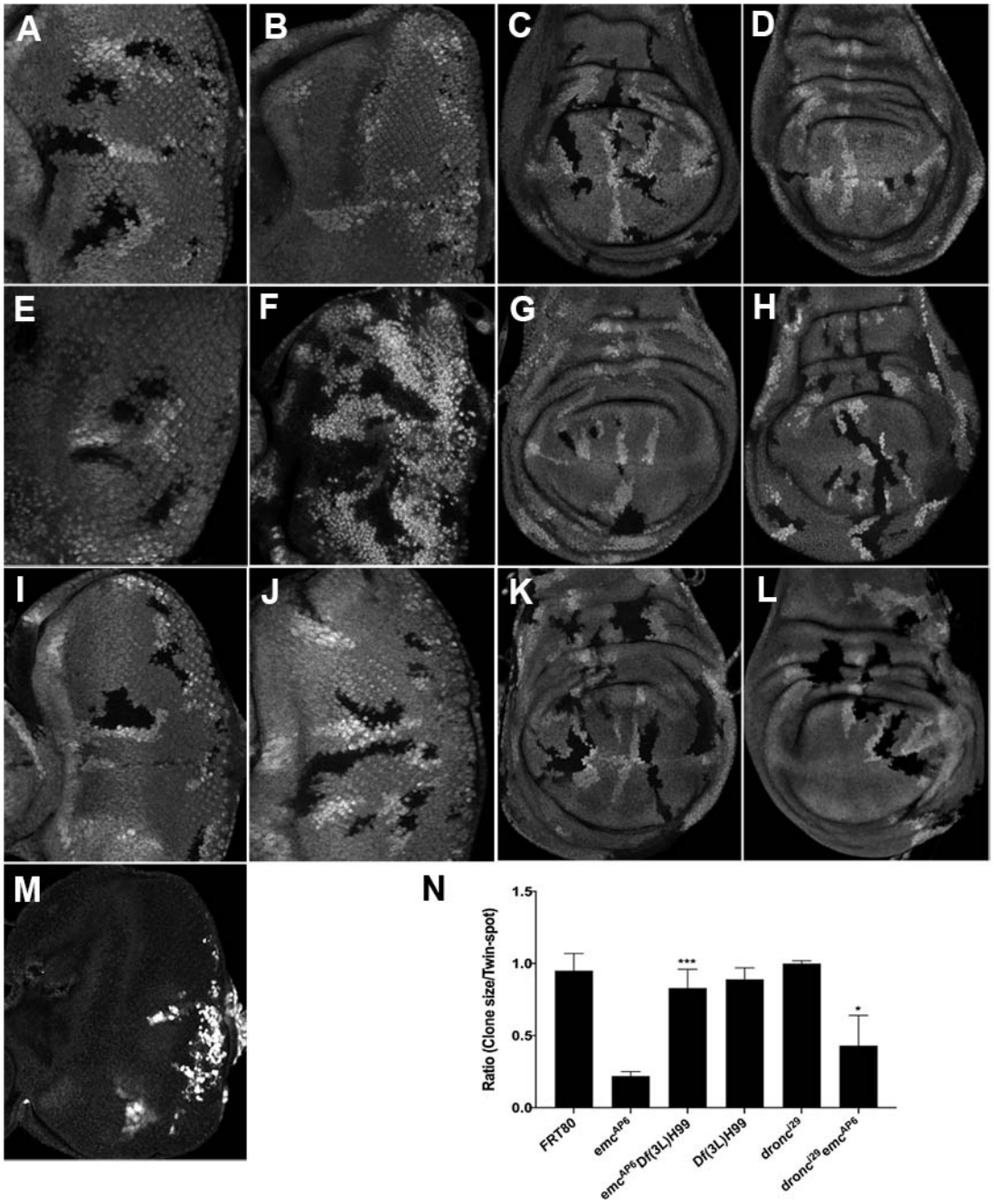

581
582 **Figure 1: *Df(3L)H99* recues growth defect in *emc* mutant**
583 (A-L) Control and mutant clones in eye and wing imaginal disc were induced at the end of first
584 instar and are associated with sibling twin-spot clones marked by two copies of the GFP marker
585 (brighter grey) that serves as internal control for growth. Clones are labeled by the absence of
586 GFP. (M) *emc H99* clones induced in the minute background (N) Quantification of the ratio of
587 clone size to twin-spot measured in wing imaginal discs and standard deviations.
588 Asterisks denote significance from *t* test (* = p<0.05, **=p<0.0, ***=p<0.001, n.s = not
589 significant). Genotypes: (A and C) *ywhsF;;FRT80/[UbiGFP]FRT80* (B and D)

590 *ywhsF;;emc^{AP6}FRT80/[Ubi-GFP]FRT80* (E and G) *ywhsF;;dronc^{i29}emc^{AP6}*
591 *FRT80/[UbiGFP]FRT80* (F and H) *ywhsF;;emc^{AP6} Df(3L)H99 FRT80/[UbiGFP]FRT80* (I and
592 K) *ywhsF;;dronc^{i29} FRT80/[UbiGFP]FRT80* (J and L)
593 *ywhsF;;Df(3L)H99FRT80/[UbiGFP]FRT80* (M) *ywhsF; emc^{AP6} Df(3L)H99 FRT80/[UbiGFP]*
594 *M(3)67C FRT80*. N=10 for each genotype.
595

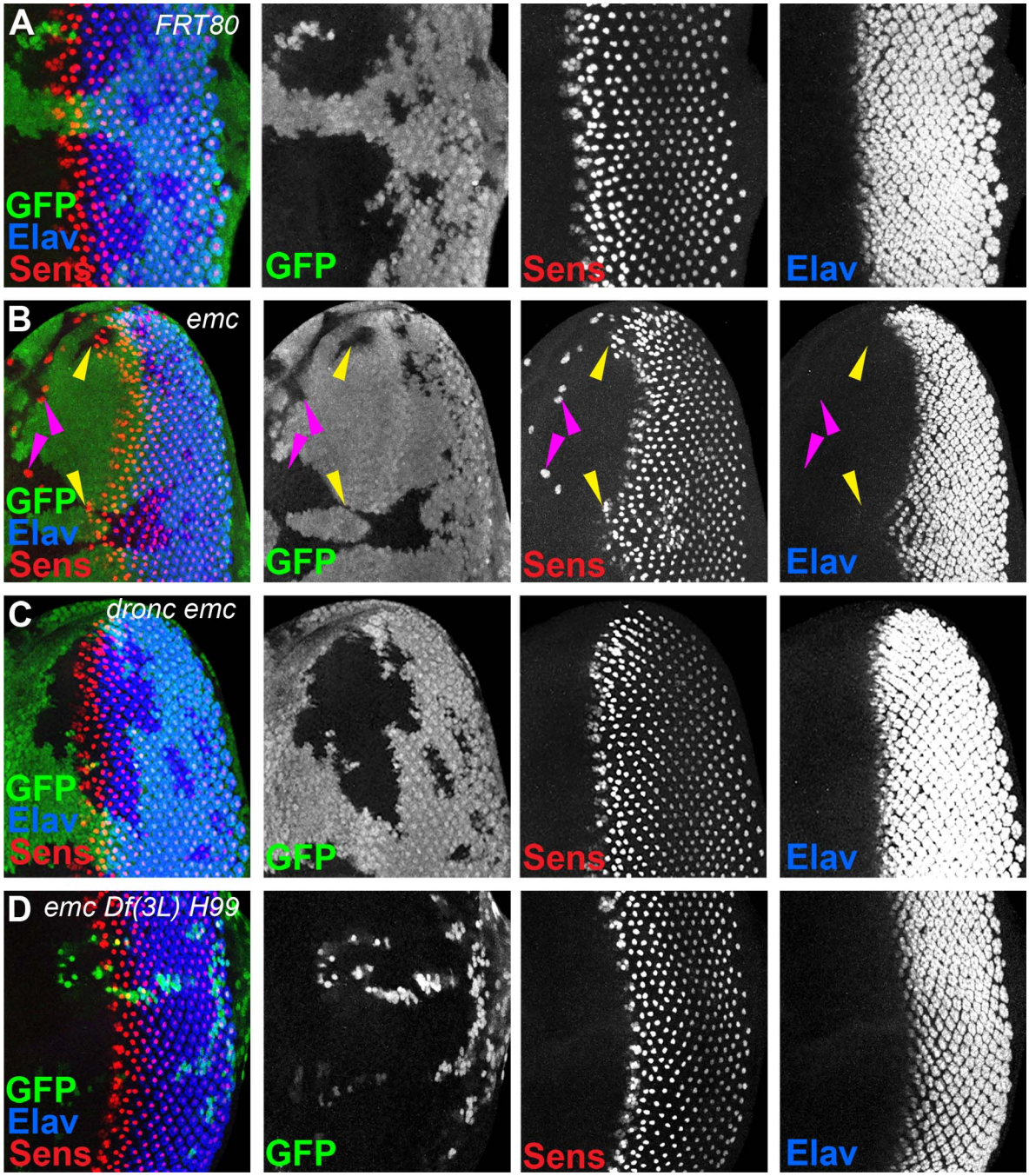

596
597 **Figure 2: Cell death signaling inhibition regulates morphogenetic furrow progression in**
598 ***emc* mutants**
599 In all panels, the differentiating neurons are marked by Elav (in blue), and mutant cells are
600 identified by the absence of GFP expression (in green). A) The wave of retinal differentiation

601 from posterior to anterior (right to left), marked here by Senseless expression in R8
602 photoreceptor cells (red) is normal in FRT80 control clones. B) *emc* null clones lacking GFP
603 show acceleration of retinal differentiation illustrated by yellow arrows (premature
604 differentiation can also continue in to wild type regions ahead of such clones). In addition,
605 ectopic neural differentiation also occurs sporadically anterior to the morphogenetic furrow, and
606 unassociated with it (magenta arrows) C) In contrast, retinal differentiation proceeds at the same
607 pace in *emc dronc* double mutant clones as in nearby wild type regions in 75% of the eye discs.
608 D) *emc H99* double mutants show a stronger suppression of the acceleration of retinal
609 differentiation (compare panel B). Genotypes: (A) *ywhsF;;FRT80/[UbiGFP] M(3)67C FRT80*
610 (B) *ywhsF;;emc^{AP6}FRT80/[Ubi-GFP] M(3)67C FRT80* (C) *ywhsF;;dronc^{i29}emc^{AP6}*
611 *FRT80/[UbiGFP] M(3)67C FRT80* (n=12)(D) *ywhsF;;emc^{AP6} Df(3L)H99 FRT80/[UbiGFP]*
612 *M(3)67C FRT80*. N=8 for each genotype.
613

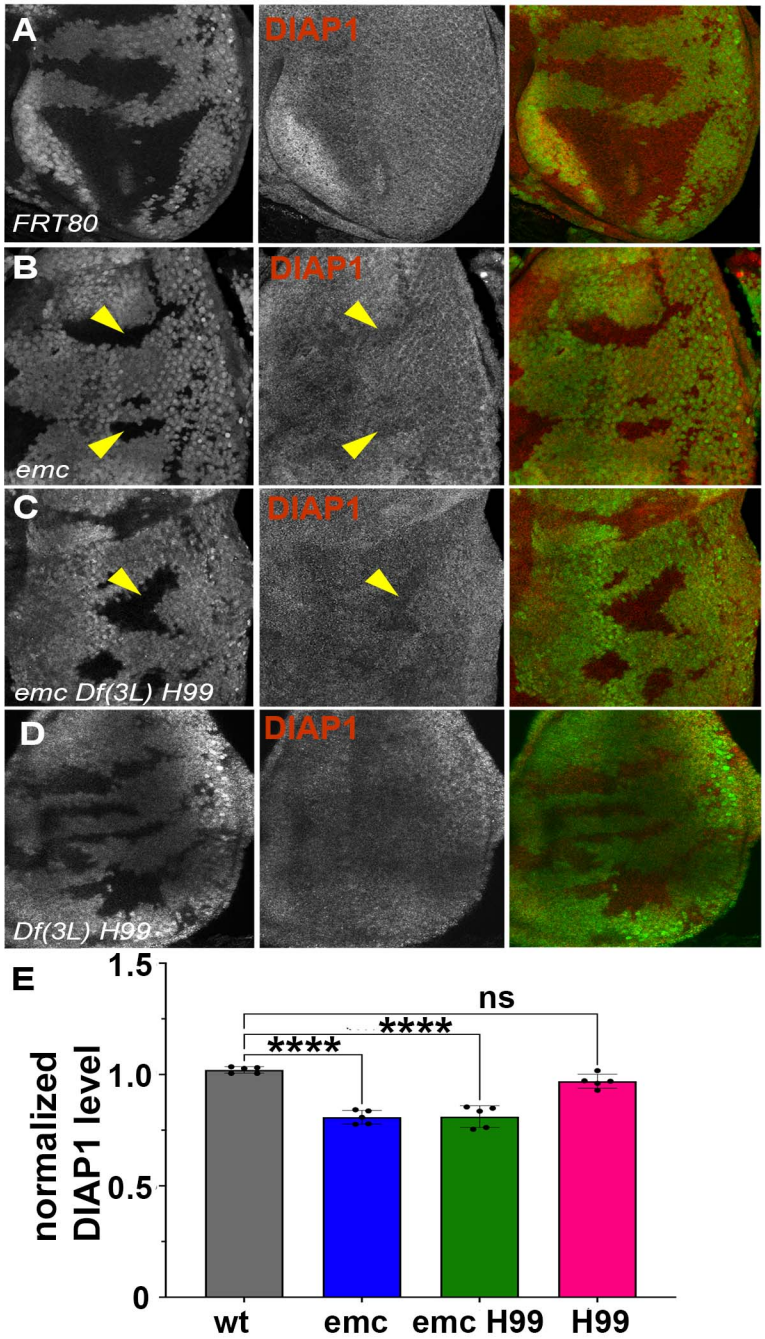

Figure 3: *Emc* mutant clones have reduced Diap1 levels

In mosaic eye discs with (A) FRT80 clones, there is no change in Diap1 levels within and outside the clone. However, both (B) *emc* mutant clones and (C) *emc H99* clones show reduced Diap1 levels posterior to the morphogenetic furrow, compared to the heterozygous background (D) *H99* clones showed similar Diap1 levels, compared to the heterozygous background. (E) Quantification of Diap1 levels in different clone genotypes, compared to the background levels outside the clones. Note that our experiments did not generate mosaics of wild type and Df(3L)H99/+ cells for direct comparison of these genotypes. Statistical significance calculated by two-way ANOVA (**$p \leq 0.01$, ***$p \leq 0.0001$). Genotypes: (A) *ywhsF;;FRT80/[UbiGFP] M(3)67C FRT80* (B) *ywhsF;;emc^{AP6}FRT80/[Ubi-GFP] M(3)67C FRT80* (C) *ywhsF;;emc^{AP6}*

625 *Df(3L)H99 FRT80/[UbiGFP] M(3)67C FRT80* (D) *ywhsF;; Df(3L)H99 FRT80/[UbiGFP]*
626 *M(3)67C FRT80.* N=6 for each genotype.
627

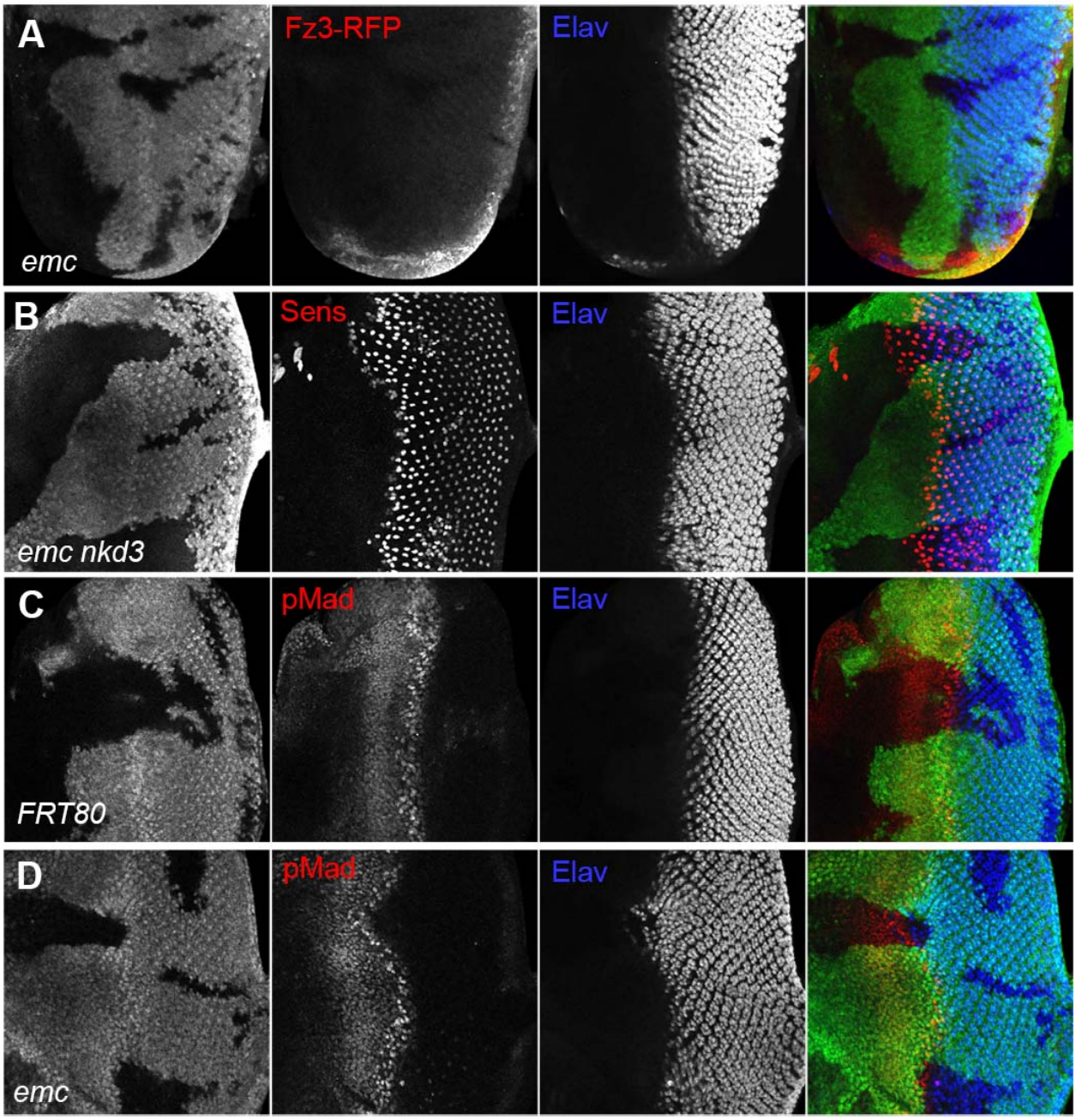

628
629 **Figure 4: Wingless and Dpp signaling are not caspase targets**
630 (A) No reduction in the Wg signaling reporter Fz3-RFP was detectable in emc clones. See
631 Figure 4 Figure Supplement 1 for Fz3-RFP expression in the wild type. (B) Retinal
632 differentiation is accelerated in *emc nkd*^{3} double mutant clones like in *emc* clones. Senseless
633 expression in R8 photoreceptor cells and Elav staining in differentiating photoreceptors are
634 shown. (C) p-Mad accumulates around the morphogenetic furrow in eye discs containing control
635 clones(Firth et al., 2010; Vrailas and Moses, 2006) (E) Except for the advanced progression, p-
636 Mad levels were unchanged in *emc* clones. Genotypes: (A) Fz3-RFP/+; *emc*^{AP6}*FRT80/[Ubi-*

637 *GFP] M(3)67C FRT80* (B) *ywhsF;;emc^{AP6}nkd^{3}FRT80/[Ubi-GFP] M(3)67C FRT80* (C)
638 *ywhsF;;FRT80/[UbiGFP] M(3)67C FRT80* (D) *ywhsF;;emc^{AP6}FRT80/[Ubi-GFP] M(3)67C*
639 *FRT80***.** N=8 for each genotype.
640

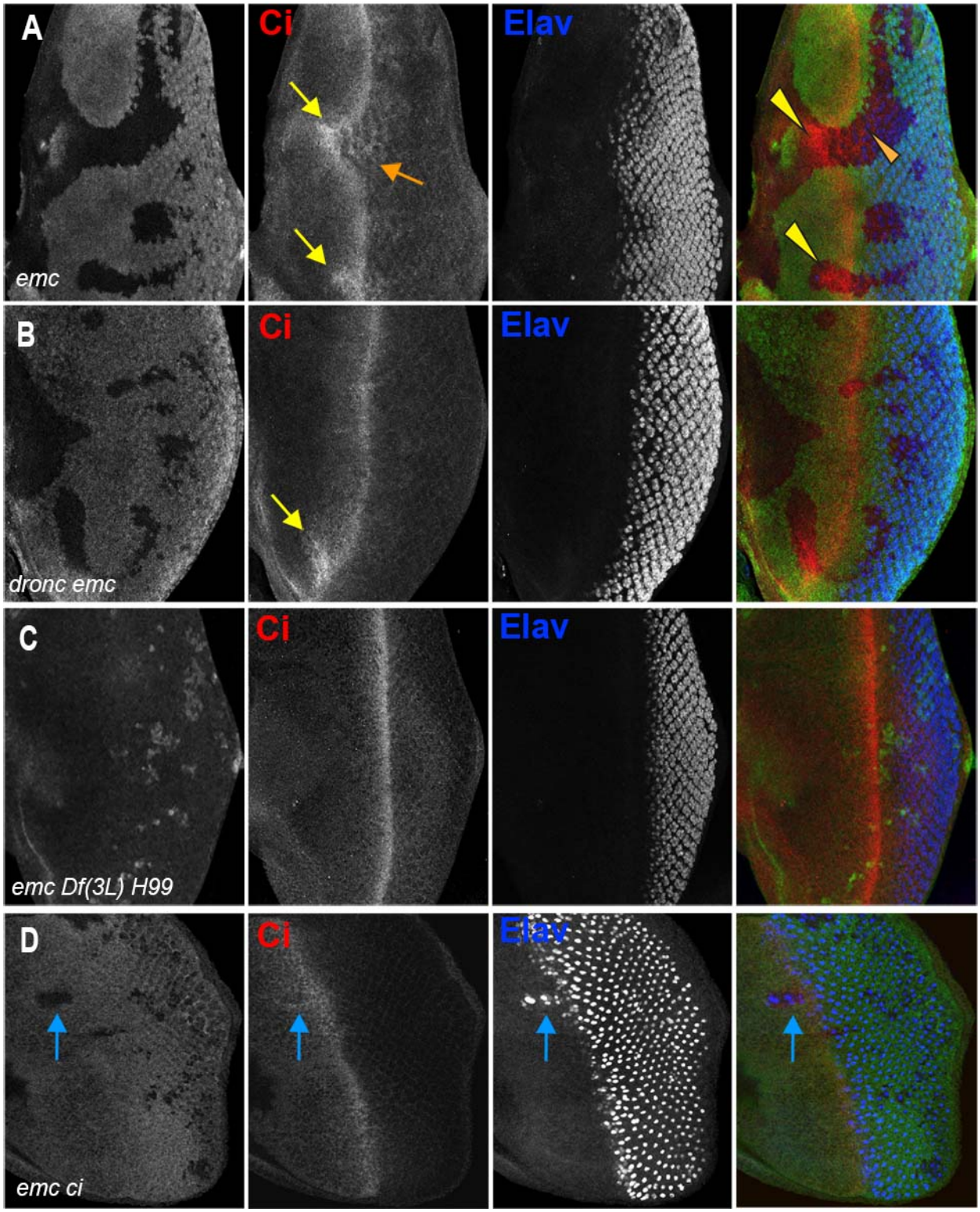

641

642 **Figure 5: *emc ci* double mutant clones with Ci transgene do not suppress morphogenetic**
643 **furrow progression**
644 A) Ci is elevated within *emc* mutant cells (yellow arrows). This was also true posterior to the
645 morphogenetic furrow (orange arrow) B) Higher Ci was also seen in *emc dronc* mutant cells,
646 even when the morphogenetic furrow progressed normally, as indicated by Elav staining. C) Ci
647 levels were completely normal in *emc H99* clones. D) *emc* and *ci* double mutant clones lacking
648 GFP shows accelerated retinal differentiation (blue arrow). Genotypes: (A)
649 *ywhsF;;emc^{AP6}FRT80/[Ubi-GFP] M(3)67C FRT80* (B) *ywhsF;;dronc^{i29}emc^{AP6}*
650 *FRT80/[UbiGFP] M(3)67C FRT80* (C) *ywhsF;;emc^{AP6} Df(3L)H99 FRT80/[UbiGFP] M(3)67C*
651 *FRT80* (D) *ywhsF;;emc^{AP6}FRT80/[Ubi-GFP] ci^{+} M(3)67C FRT80;ci[94]/ci[94].* N=8 for each
652 genotype except (D) which has n=3.
653

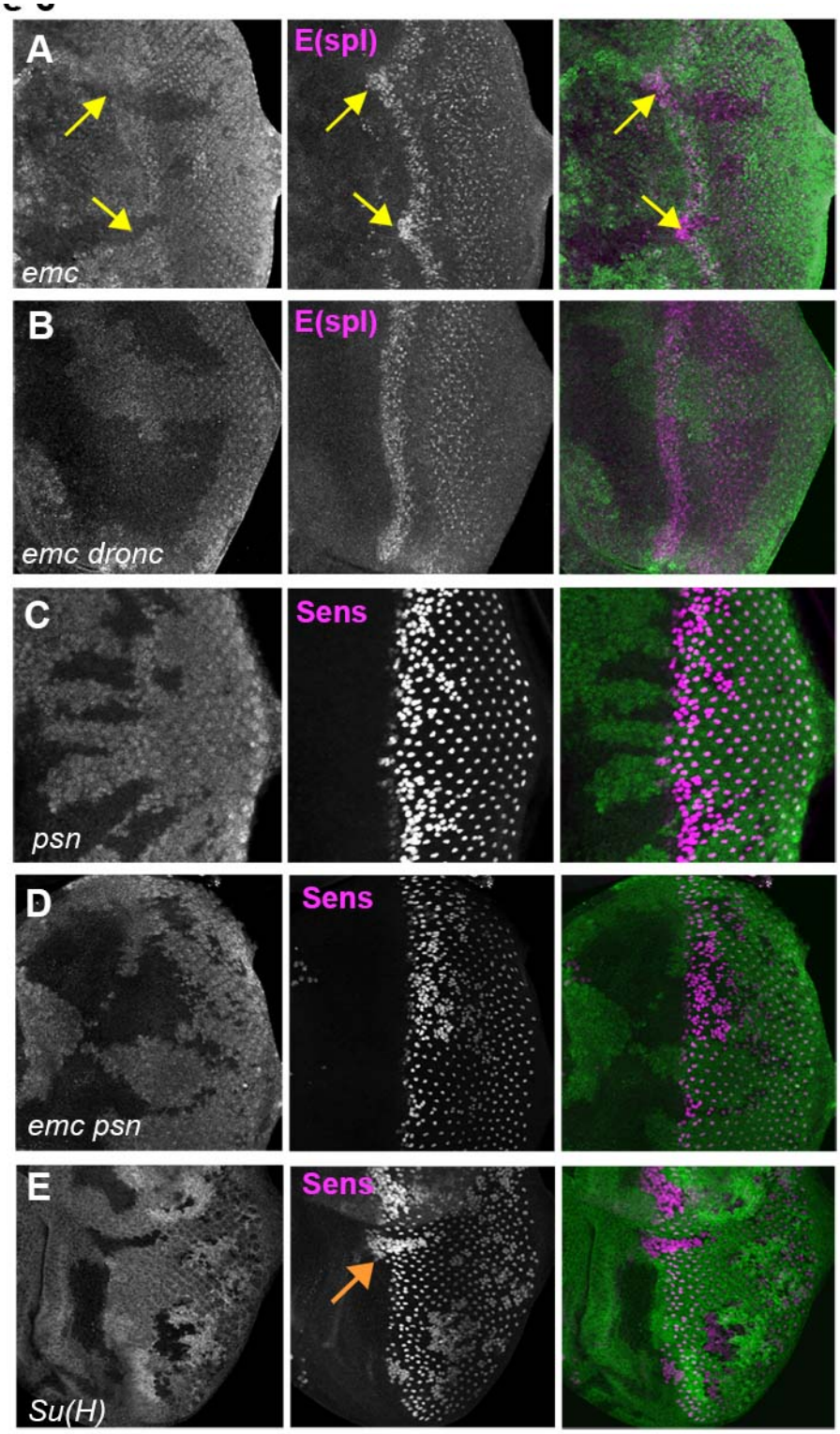

Figure 6: Notch activity and function in emc mutant clones.
(A) E(spl), an important N target for lateral inhibition, is elevated in the morphogenetic furrow region of *emc* clones (yellow arrows). (B) *emc dronc* clones have normal levels of E(spl) protein. (C) Senseless staining shows a neurogenic phenotype in *psn* mutant clones, due to reduced Notch signaling. Morphogenetic furrow progression is unaffected. (D) A neurogenic phenotype was

also observed in *emc psn* clones, along with normal furrow progression. (E) *Su(H)* mutant clones identified by absence of GFP labeling show a strong neurogenic phenotype as well as advanced retinal differentiation (orange arrow) (Li and Baker, 2001). The cell-autonomous effect results in a discontinuity at the borders of *Su(H)* clones, where differentiation outside the clones lags that within clones (orange arrow) Genotypes: (A) *ywhsF;;emc*^{AP6} *FRT80/[Ubi-GFP] M(3)67C FRT80* (B) *ywhsF;; dronc*^{i29}*emc*^{AP6} *FRT80/[UbiGFP] M(3)67C FRT80* (C) *ywhsF/+;;psn*^{V1} *FRT80/[Ubi-GFP]M(3)67CFRT80* (D) *ywhsF/+;; emc*^{AP6} *psn*^{V1} *FRT80/[Ubi-GFP]M(3)67CFRT80* ((E) *ywhsF; Su(H)*^{D47}FRT40/FRT40*[UbiGFP]*. N=6 for each genotype.

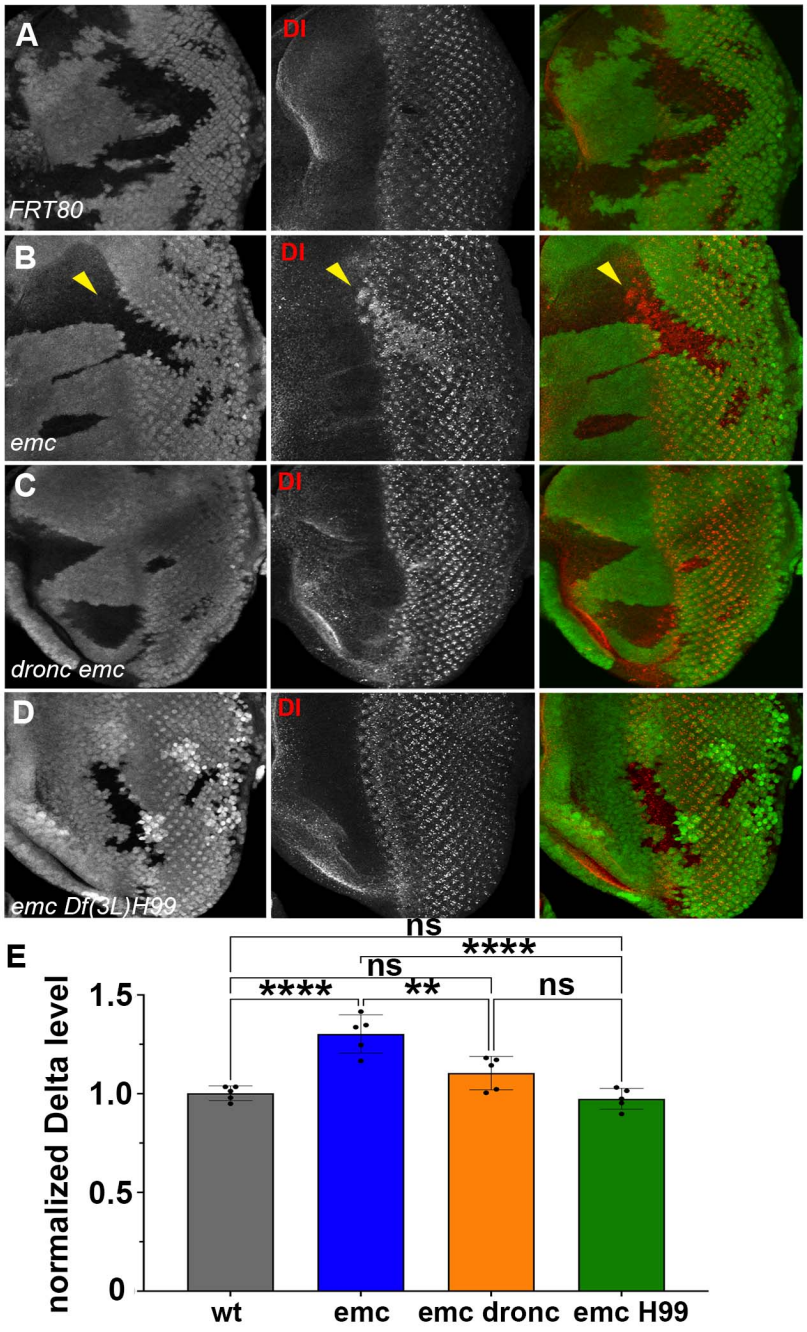

Figure 7: Caspases regulate Delta levels

671 (A) Normal levels of Delta protein are seen in FRT80 clones as compared to elevated Delta
672 levels in (B) *emc* clones whereas that phenotype is reversed in (D) *emc H99* clones. However, as
673 seen in (C) Some *dronc emc* clones show intermediate Delta levels. (E) Quantification of Delta
674 levels in different clone genotypes, compared to the background levels outside the clones.
675 Genotypes: (A) *ywhsF;;FRT80/[UbiGFP] M(3)67C FRT80* (B) *ywhsF;;emc*^{AP6}*FRT80/[Ubi-*
676 *GFP] M(3)67C FRT80* (C) *ywhsF;;dronc*^{i29}*emc*^{AP6} *FRT80/[UbiGFP] M(3)67C FRT80* (D)
677 *ywhsF;;emc*^{AP6} *Df(3L)H99 FRT80/[UbiGFP]FRT80*. N=7 for each genotype. Significance was
678 determined using one-way Anova with Tukey's post-hoc test.
679

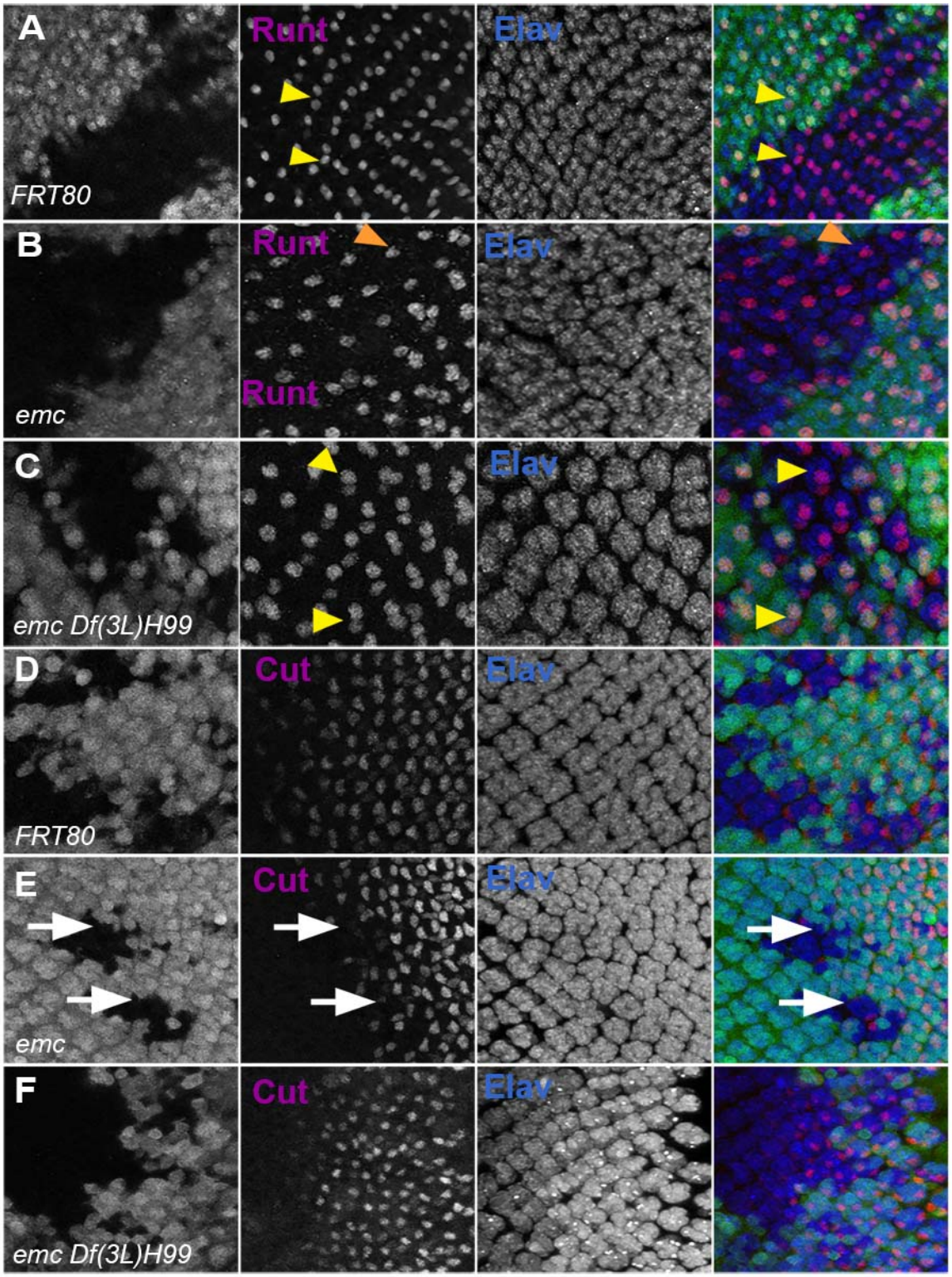

Figure 8: Caspases partially rescue defects in R7 photoreceptor and cone cell differentiation in emc mutants

In all panels *emc* mutant cells are marked by the absence of GFP expression (in green) and photoreceptor neurons are marked by Elav in blue. (A) Runt (in red) is expressed in R7 and R8 (yellow arrowhead) photoreceptor cells inside and outside the clone in FRT80 controls. (B)

686 Inside *emc* clone, Runt expression is lost from R7 cells, while expression in R8 cells remains
687 unaffected (red arrow). (C) However, inside the *emc H99* clones, Runt is expressed in both R7
688 and R8 cells. (D) Cut (in red) is expressed in cone cells in FRT80 controls. (E) Inside *emc* clone,
689 cut is delayed. (F) However, inside the *emc H99* clones, cut staining is not delayed. Genotypes:
690 (A, D) *ywhsF;;FRT80/[UbiGFP] M(3)67C FRT80* (B, E) *ywhsF;;emc*^{AP6}*FRT80/[Ubi-GFP]*
691 *M(3)67C FRT80* (C, F) *ywhsF;;emc*^{AP6} *Df(3L)H99 FRT80/[UbiGFP] M(3)67C FRT80*. N=4 for
692 each genotype.
693

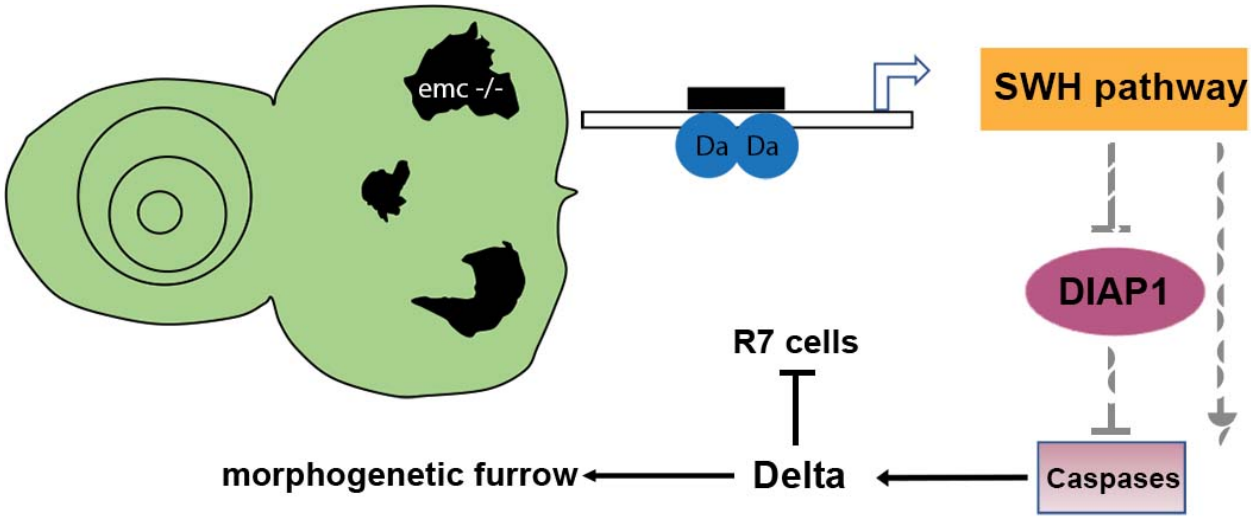

694
695 **Figure 9: Model of *emc* effects on *Drosophila* eye development.** Loss of *emc* allows Da
696 protein to form heterodimers and activate *ex* transcription, increasing SWH pathway activity.
697 SWH activity reduces DIAP1 expression, thereby derepressing caspase activity. In the eye, non-
698 apoptotic caspase activity increases expression of the Notch ligand Delta. Elevated Delta
699 expression accelerates morphogenetic furrow progression, while cis-inhibiting Notch signaling
700 posterior to the morphogenetic furrow, inhibiting R7 cell specification and cone-cell
701 differentiation. In wild type cells, most Da is likely heterodimerized with either a proneural
702 protein or with Emc protein, and there is no role of caspases in Dl expression.
703

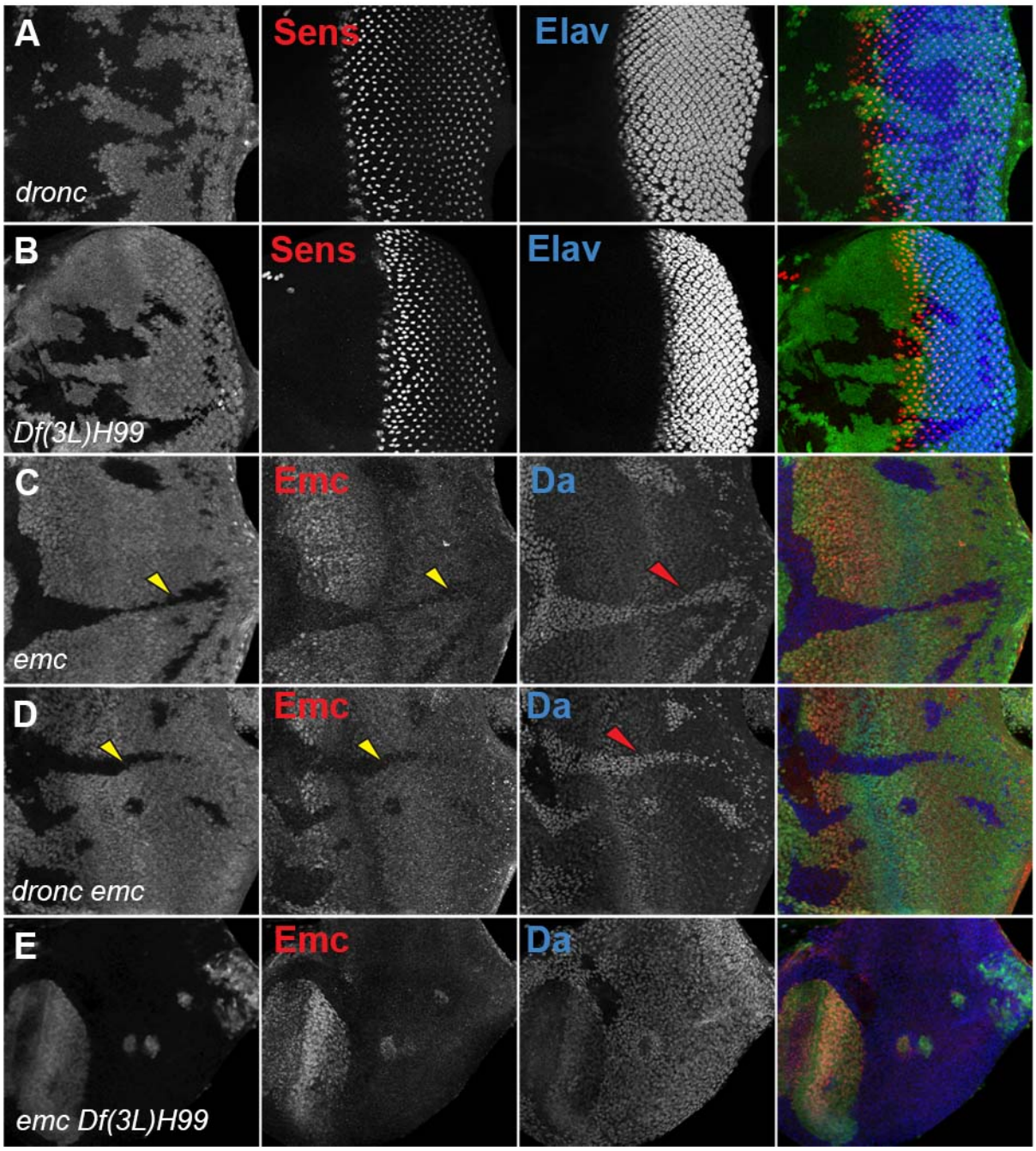

Figure 2 Figure Supplement 1: Morphogenetic furrow progression in *emc* mutant cells
In eye imaginal discs, normal furrow progression was observed in (A) *dronc* $^{-/-}$ and (B) *Df(3L)H99* homozygous clones, indicated by Senseless and Elav staining. Homozygous mutant clones of *emc*$^{-/-}$ (C) lacking GFP expression, have no Emc staining (yellow arrowhead) and higher Da (red arrowhead). At the morphogenetic furrow as shown by yellow arrow, Emc expression goes down and Da goes up. Similar results were observed in (D) *dronc*$^{-/-}$ *emc*$^{-/-}$ clones and (E) *emc*$^{-/-}$ *Df(3L) H99* $^{-/-}$ clones confirm that these are *emc* null clones. Genotypes: (A) *ywhsF;;dronc*^{i29}*FRT80/[UbiGFP] M(3)67C FRT80* (B) *ywhsF;; Df(3L)H99 FRT80/[UbiGFP] M(3)67C FRT80*. (C) *ywhsF;;emc*^{AP6}*FRT80/[Ubi-GFP] M(3)67C FRT80* (D)

714 *ywhsF;;dronc*^{i29}*emc*^{AP6} *FRT80/[UbiGFP] M(3)67C FRT80* (E) *ywhsF;;emc*^{AP6} *Df(3L)H99*
715 *FRT80/[UbiGFP] M(3)67C FRT80*. N=4 for each genotype.

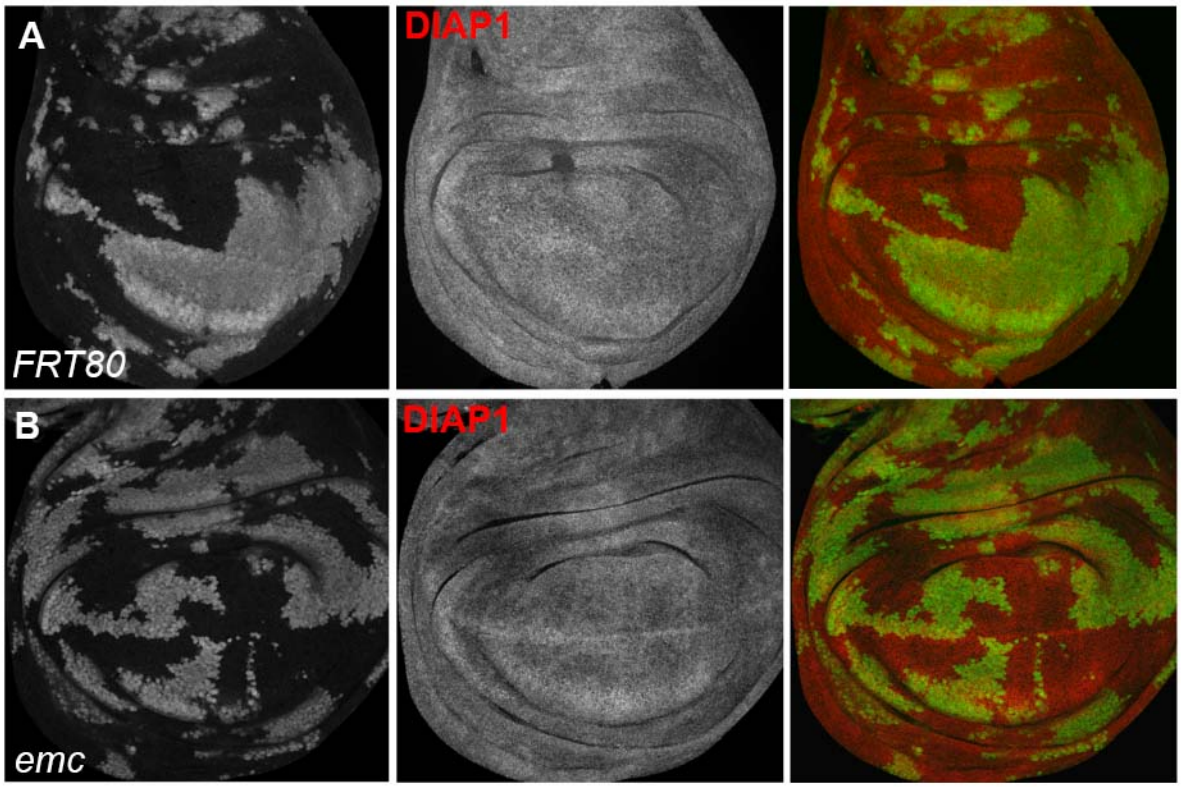

716
717 **Figure 3 Figure Supplement 1: DIAP1 staining in wing disc clones.** In wing discs of emc
718 clones (B) we did not detect changes in Diap1 levels in comparison to control clones (A).
719 Genotypes: (A) *ywhsF;;FRT80/[UbiGFP] M(3)67C FRT80* (B) *ywhsF;;emc*^{AP6}*FRT80/[Ubi-*
720 *GFP] M(3)67C FRT80.*
721
722
723
724
725
726
727
728
729
730
731
732

Figure 3 Supplement 2

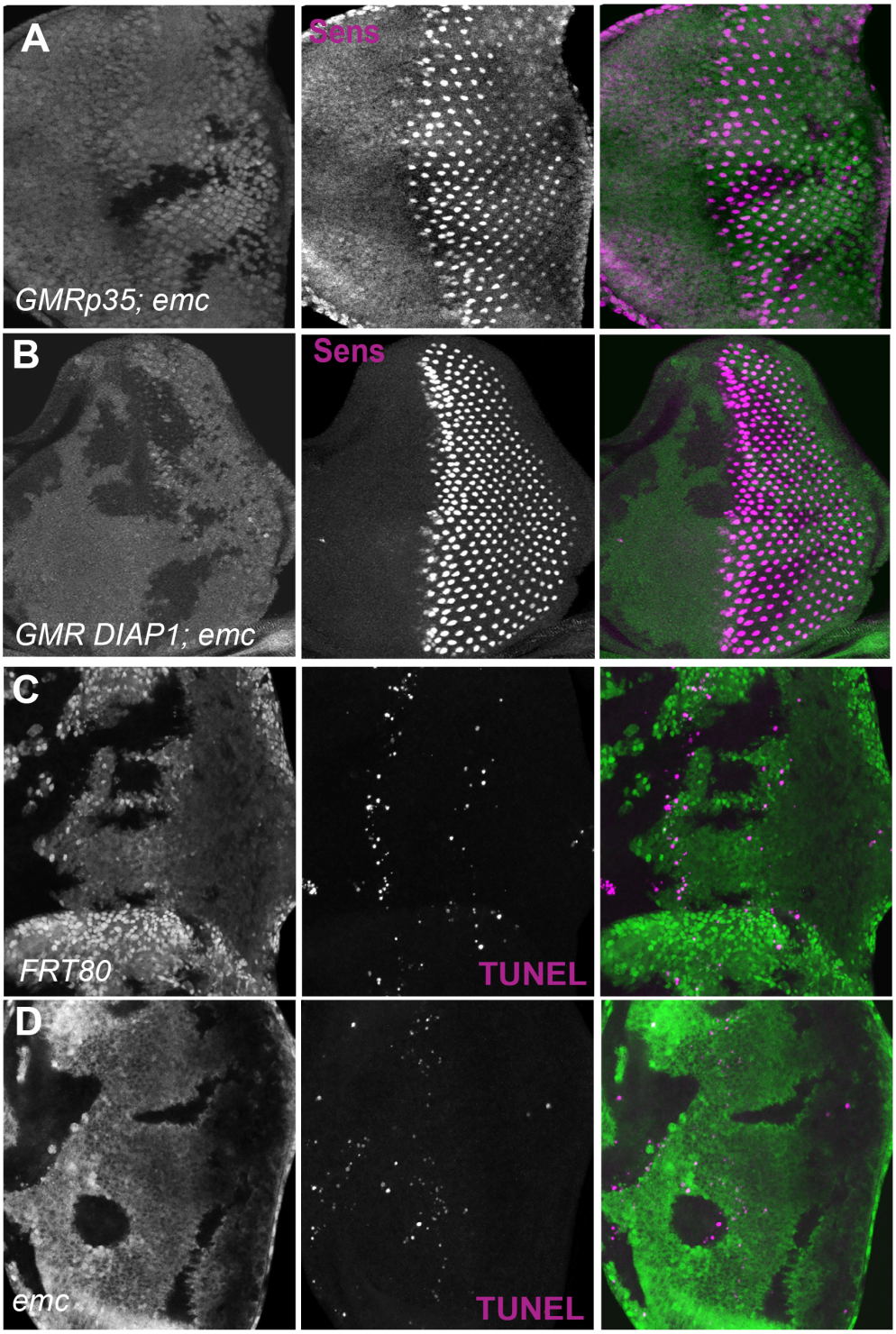

733
734

735 **Figure 3 Figure Supplement 2: Apoptosis and furrow progression** Representative images of
736 eye imaginal discs stained for senseless. (A) In GMR-DIAP1 eye disc mutant for emc furrow
737 progression is normal and is marked by Senseless staining. Similarly, in GMR-p35 eye disc
738 mutant for emc also show normal furrow progression (B). Representative images of eye imaginal
739 discs with TUNEL staining. (A) ywhsF/GMR-DIAP1;;*emc*^{AP6}*FRT80/[Ubi-GFP] M(3)67C*
740 *FRT80* B) ywhsF/GMR-p35;;*emc*^{AP6}*FRT80/[Ubi-GFP] M(3)67C FRT80*. (C)
741 *ywhsF;;FRT80/[UbiGFP] M(3)67C FRT80* (D) *ywhsF;;emc*^{AP6}*FRT80/[Ubi-GFP] M(3)67C*
742 *FRT80*. N=4 for each genotype.
743

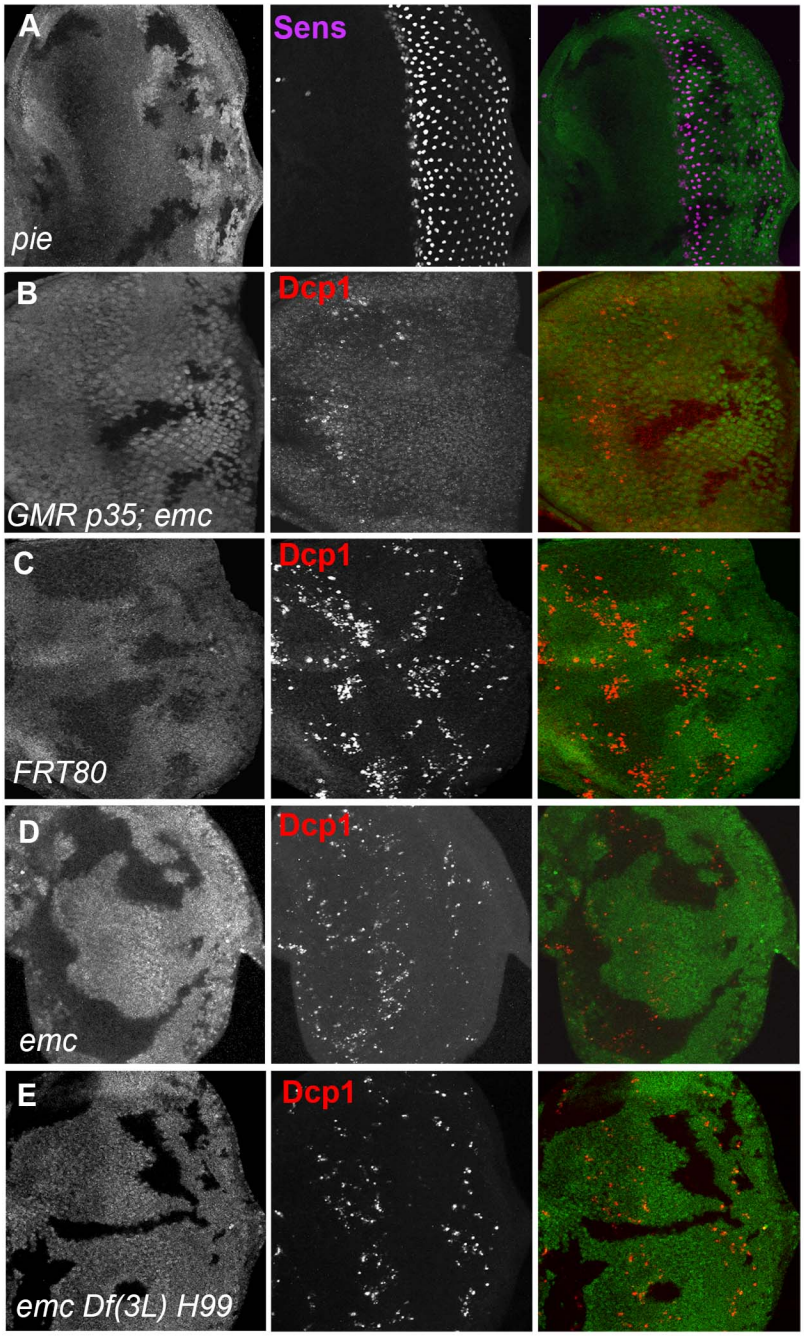

744

745 **Figure 3 Figure Supplement 3: Emc clones show no caspase activity beyond the**
746 **morphogenetic furrow.** In *pie*^{EB3} homozygous clones, furrow progression occurs at normal
747 speed marked by Senseless staining in R8 photoreceptors (A). In GMR-p35 eye disc mutant for
748 emc show lack of Dcp1staining (B). In *emc* mutant clones posterior to morphogenetic furrow
749 show lack of Dcp1 staining (D) in comparison to FRT80 clones (C). Genotypes: (A) ywhsF/+;
750 *pie*^{EB3}*FRT40/FRT40Alz*. **(B)** ywhsF/GMR-p35;;*emc*^{AP6}*FRT80/[Ubi-GFP] M(3)67C FRT80* (C)
751 *ywhsF;;FRT80/[UbiGFP] M(3)67C FRT80* (D) *ywhsF;;emc*^{AP6}*FRT80/[Ubi-GFP] M(3)67C*
752 *FRT80*. (E) *ywhsF;;emc*^{AP6} *Df(3L)H99 FRT80/[UbiGFP] M(3)67C FRT80*. N=4 for each
753 genotype.
754
755

Figure 4 figure supplement 1

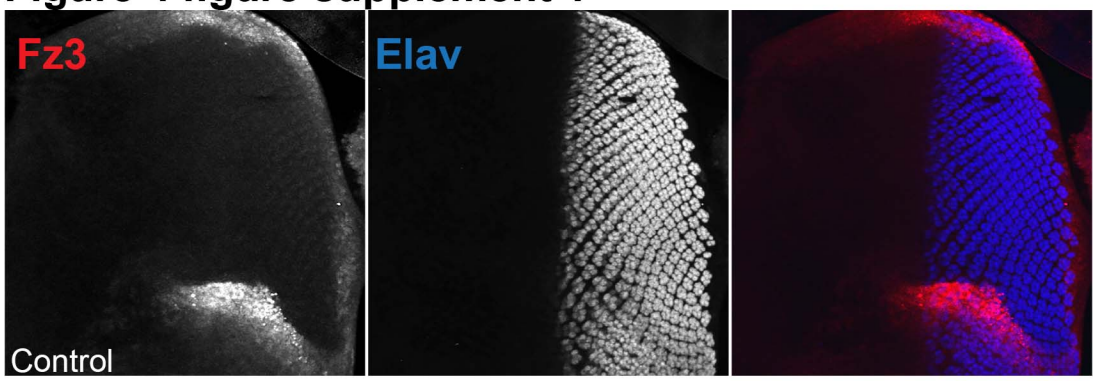

756
757 **Figure 4 Figure Supplement 1:** Fz3-RFP/+ eye disc showing RFP and Elav staining. N=3.
758

Figure 5 figure supplement 1

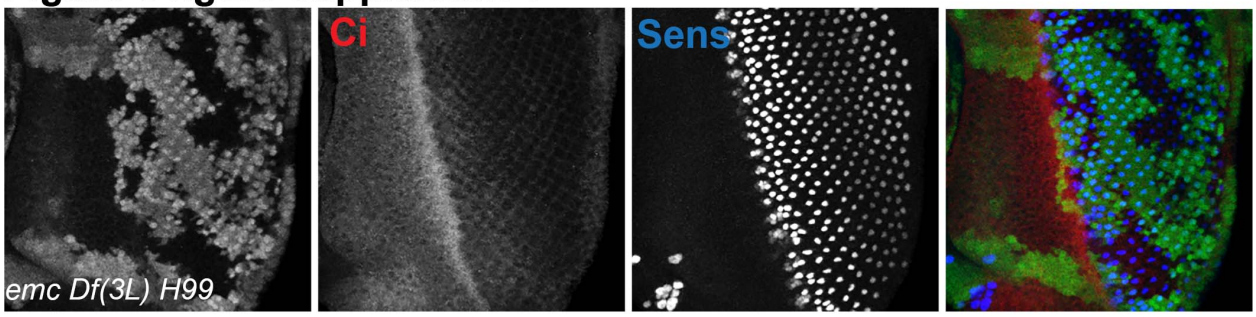

759
760 **Figure 5 Figure Supplement 1: Ci155 levels when cell death pathways are blocked**
761 Representative image of eye imaginal disc in *emc H99* clones in the non-Minute background,
762 showing similar areas inside and outside clones. Genotype: *ywhsF;; emc*^{AP6} *Df(3L)H99*
763 *FRT80/[UbiGFP]FRT80.* N=4.
764

Figure 5 Figure Supplement 2

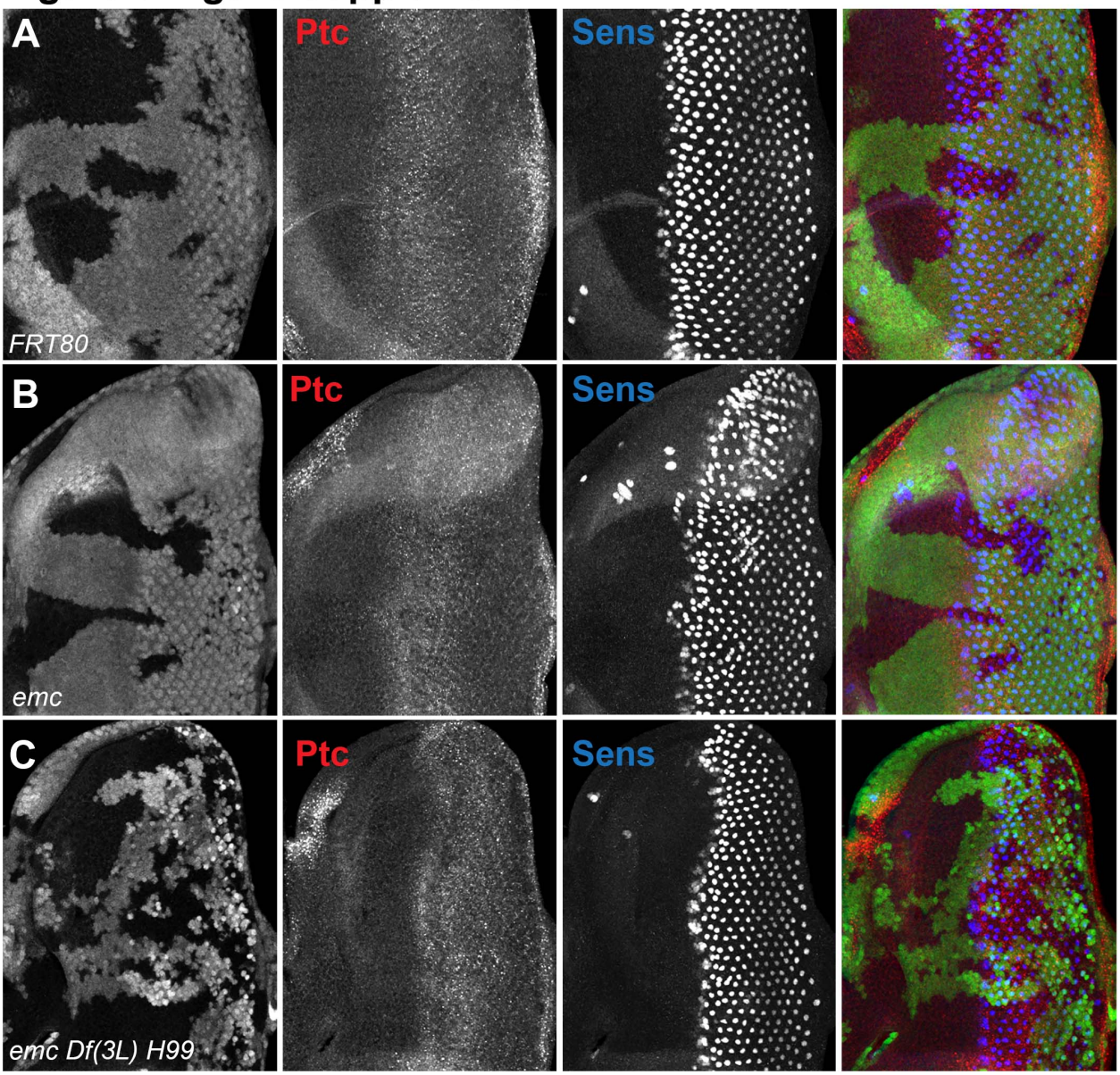

765
766 **Figure 5 Figure Supplement 2: Patched staining in emc mutants**
767 (A) *ywhsF;;FRT80/[UbiGFP] M(3)67C FRT80* (B) *ywhsF;;emc^{AP6}FRT80/[Ubi-GFP]*
768 *M(3)67C FRT80* (C) *ywhsF;;emc^{AP6} Df(3L)H99 FRT80/[UbiGFP] M(3)67C FRT8.*
769
770

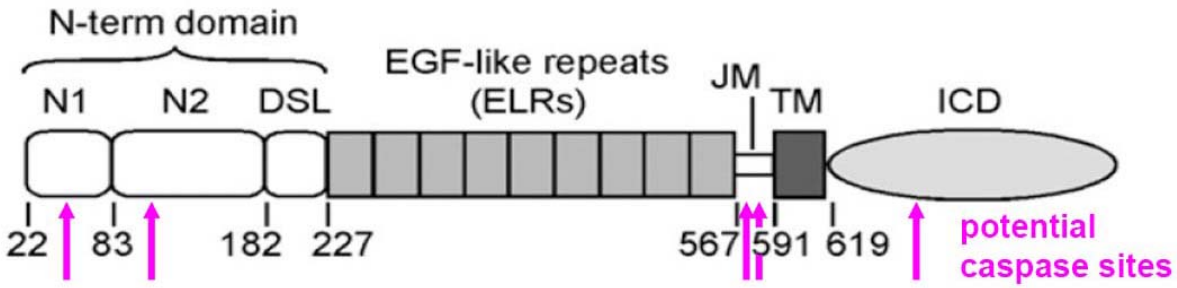

Figure 7 Figure Supplement 1: Potential Caspase sites predicted in the Delta protein. Like many proteins, Delta has multiple potential caspase cleavage sites, here predicted suing Cascleave 2.0 (Wang et al., 2014). None are high-confidence predictions and only one is in the intracellular domain where caspase access is plausible (position 675, predicted score 0.647). The intracellular domain is required for Delta signaling. Cleavage at position 675 would remove the main ubiquitylation site required for signaling, as well as the binding site for *mindbomb*, so is not anticipated to enhance signaling activity (Daskalaki et al., 2011).

781 **References**
782
783 Adam, J.C., and Montell, D.J. (2004). A role for extra macrochaetae downstream of Notch in
784 follicle cell differentiation. Development *131*, 5971-5980.
785 Andrade-Zapata, I., and Baonza, A. (2014). The bHLH factors extramacrochaetae and
786 daughterless control cell cycle in Drosophila imaginal discs through the transcriptional
787 regulation of the Cdc25 phosphatase string. PLoS Genet *10*, e1004233.
788 Aram, L., Yacobi-Sharon, K., and Arama, E. (2017). CDPs: caspase-dependent non-lethal
789 cellular processes. Cell Death Differ *24*, 1307-1310.
790 Aza-Blanc, P., Ramirez-Weber, F.A., Laget, M.P., Schwartz, C., and Kornberg, T.B. (1997).
791 Proteolysis that is inhibited by hedgehog targets Cubitus interruptus protein to the nucleus and
792 converts it to a repressor. Cell *89*, 1043-1053.
793 Baena-Lopez, L.A., Arthurton, L., Xu, D.C., and Galasso, A. (2018). Non-apoptotic Caspase
794 regulation of stem cell properties. Semin Cell Dev Biol *82*, 118-126.
795 Baker, N.E. (1988). Transcription of the segment-polarity gene wingless in the imaginal discs of
796 Drosophila, and the phenotype of a pupal-lethal wg mutation. Development *102*, 489-497.
797 Baker, N.E., Bhattacharya, A., and Firth, L.C. (2009). Regulation of Hh signal transduction as
798 Drosophila eye differentiation progresses. Dev Biol *335*, 356-366.
799 Baker, N.E., Li, K., Quiquand, M., Ruggiero, R., and Wang, L.H. (2014). Eye development.
800 Methods *68*, 252-259.
801 Baker, N.E., Moses, K., Nakahara, D., Ellis, M.C., Carthew, R.W., and Rubin, G.M. (1992).
802 Mutations on the second chromosome affecting the Drosophila eye. J Neurogenet *8*, 85-100.
803 Baker, N.E., and Yu, S.Y. (1998). The R8-photoreceptor equivalence group in *Drosophila* : fate
804 choice precedes regulated *Delta* transcription and is independent of *Notch* gene dose.
805 Mechanisms of Development *74*, 3-14.
806 Baonza, A., and Freeman, M. (2001a). Notch signalling and the initiation of neural development
807 in the *Drosophila* eye. Development *128*, 3889-3898.
808 Baonza, A., and Freeman, M. (2001b). Notch signalling and the initiation of neural development
809 in the Drosophila eye. Development *128*, 3889-3898.
810 Benezra, R., Davis, R.L., Lockshon, D., Turner, D.L., and Weintraub, H. (1990). The protein Id:
811 a negative regulator of helix-loop-helix DNA binding proteins. Cell *61*, 49-59.
812 Bhattacharya, A., and Baker, N.E. (2009). The HLH protein Extramacrochaetae is required for
813 R7 cell and cone cell fates in the Drosophila eye. Dev Biol *327*, 288-300.
814 Bhattacharya, A., and Baker, N.E. (2011). A network of broadly expressed HLH genes regulates
815 tissue-specific cell fates. Cell *147*, 881-892.
816 Bhattacharya, A., and Baker, N.E. (2012). The Role of the bHLH Protein Hairy in
817 Morphogenetic Furrow Progression in the Developing Drosophila Eye. PLoS One *7*, e47503.
818 Borod, E.R., and Heberlein, U. (1998). Mutual regulation of decapentaplegic and hedgehog
819 during the initiation of differentiation in the Drosophila retina. Dev Biol *197*, 187-197.
820 Bray, S.J. (2006). Notch signalling: a simple pathway becomes complex. Nat Rev Mol Cell Biol
821 *7*, 678-689.
822 Bray, S.J. (2016). Notch signalling in context. Nat Rev Mol Cell Biol *17*, 722-735.
823 Brown, N.L., Paddock, S.W., Sattler, C.A., Cronmiller, C., Thomas, B.J., and Carroll, S.B.
824 (1996). *daughterless* is required for *Drosophila* photoreceptor cell determination, eye
825 morphogenesis, and cell cycle progression. Developmental Biology *179*, 65-78.

826 Brown, N.L., Sattler, S.A., Paddock, S.W., and Carroll, S.B. (1995). *hairy* and *emc* negatively
827 regulate morphogenetic furrow progression in the developing *Drosophila* eye. Cell *80*, 879-887.
828 Cabrera, C.V., Alonso, M.C., and Huikeshoven, H. (1994). Regulation of scute function by
829 extramacrochaete in vitro and in vivo. Development *120*, 3595-3603.
830 Cadigan, K.M., Jou, A.D., and Nusse, R. (2002). Wingless blocks bristle formation and
831 morphogenetic furrow progression in the eye through repression of Daughterless. Development
832 *129*, 3393-3402.
833 Chang, J.L., Chang, M.V., Barolo, S., and Cadigan, K.M. (2008). Regulation of the feedback
834 antagonist naked cuticle by Wingless signaling. Dev Biol *321*, 446-454.
835 Coelho, C.M., Kolevski, B., Bunn, C., Walker, C., Dahanukar, A., and Leevers, S.J. (2005).
836 Growth and cell survival are unevenly impaired in pixie mutant wing discs. Development *132*,
837 5411-5424.
838 Colon-Plaza, S., and Su, T.T. (2022). Non-Apoptotic Role of Apoptotic Caspases in the
839 Drosophila Nervous System. Front Cell Dev Biol *10*, 839358.
840 Cooper, M.T.D., and Bray, S.J. (2000). R7 photoreceptor specification requires N activity.
841 Current Biology *10*, 1507-1510.
842 Daskalaki, A., Shalaby, N.A., Kux, K., Tsoumpekos, G., Tsibidis, G.D., Muskavitch, M.A., and
843 Delidakis, C. (2011). Distinct intracellular motifs of Delta mediate its ubiquitylation and
844 activation by Mindbomb1 and Neuralized. J Cell Biol *195*, 1017-1031.
845 Ellis, H.M. (1994). Embryonic expression and function of the Drosophila helix-loop-helix gene,
846 extramacrochaetae. Mech Dev *47*, 65-72.
847 Ellis, H.M., Spann, D.R., and Posakony, J.W. (1990). extramacrochaetae, a negative regulator of
848 sensory organ development in Drosophila, defines a new class of helix-loop-helix proteins. Cell
849 *61*, 27-38.
850 Firth, L.C., Bhattacharya, A., and Baker, N.E. (2010). Cell cycle arrest by a gradient of Dpp
851 signaling during Drosophila eye development. BMC Dev Biol *10*, 28.
852 Flores, G., Duan, H., Yan, H., Nagaraj, R., Fu, W., Zou, Y., Noll, M., and Banerjee, U. (2000).
853 Combinatorial signaling in the specification of unique cell fates. Cell *103*, 75-85.
854 Fu, W., and Baker, N.E. (2003). Deciphering synergistic and redundant roles of Hedgehog,
855 Decapentaplegic and Delta that drive the wave of differentiation in Drosophila eye development.
856 Development *130*, 5229-5239.
857 Fuchs, Y., and Steller, H. (2011). Programmed cell death in animal development and disease.
858 Cell *147*, 742-758.
859 Garcia-Alonso, L., and Garcia-Bellido, A. (1988). Extramacrochaetae a trans-acting gene of the
860 Achaete-Scyte complex of *Drosophila* involved in cell communication. Roux's Archives of
861 Developmental Biology *197*, 328-338.
862 Garrell, J., and Modolell, J. (1990). The Drosophila extramacrochaetae locus, an antagonist of
863 proneural genes that, like these genes, encodes a helix-loop-helix protein. Cell *61*, 39-48.
864 Golic, K.G. (1991). Site-specific recombination between homologous chromosomes in
865 Drosophila. Science *252*, 958-961.
866 Hawkins, C.J., Yoo, S.J., Peterson, E.P., Wang, S.L., Vernooy, S.Y., and Hay, B.A. (2000a). The
867 Drosophila caspase DRONC cleaves following glutamate or aspartate and is regulated by
868 DIAP1, HID, and GRIM. J Biol Chem *275*, 27084-27093.
869 Hawkins, C.J., Yoo, S.J., Peterson, E.P., Wang, S.L., Vernooy, S.Y., and Hay, B.A. (2000b). The
870 *Drosophila*caspase DRONC cleaves following glutamate or aspartate and is regulated by DIAP1,
871 HID, and GRIM. Journal of Biological Chemistry *275*, 27084-27093.

872 Hay, B.A., Wolff, T., and Rubin, G.M. (1994). Expression of baculovirus P35 prevents cell death
873 in *Drosophila*. Development *120*, 2121-2129.
874 Heberlein, U., Singh, C.M., Luk, A.Y., and Donohoe, T.J. (1995). Growth and differentiation in
875 the *Drosophila* eye coordinated by *hedgehog*. Nature *373*, 709-711.
876 Heberlein, U., Wolff, T., and Rubin, G.M. (1993a). The TGF beta homolog dpp and the segment
877 polarity gene hedgehog are required for propagation of a morphogenetic wave in the Drosophila
878 retina. Cell *75*, 913-926.
879 Heberlein, U., Wolff, T., and Rubin, G.M. (1993b). The TGF-ß homolog *dpp* and the segment
880 polarity gene *hedgehog* are required for propagation of a morphogenetic wave in the *Drosophila*
881 retina. Cell *75*, 913-926.
882 Hepker, J., Wang, Q.-T., Motzny, C., Holmgren, R., and Orenic, T.V. (1997). *Drosophila cubitus*
883 *interruptus* forms a negative feedback loop with *patched* and regulates expression of Hedgehog
884 target genes. Development *124*, 549-558.
885 Jacobsen, T.L., Brennan, K., Martinez-Arias, A., and Muskavitch, M.A. (1998). Cis-interactions
886 between Delta and Notch modulate neurogenic signalling in *Drosophila*. Development *125*,
887 4531-4540.
888 Jarman, A.P., Grell, E.H., Ackerman, L., Jan, L.Y., and Jan, Y.N. (1994). *atonal* is the proneural
889 gene for *Drosophila* photoreceptors. Nature *369*, 398-400.
890 Jennings, B., Preiss, A., Delidakis, C., and Bray, S. (1994). The Notch signalling pathway is
891 required for Enhancer of split bHLH protein expression during neurogenesis in the Drosophila
892 embryo. Development *120*, 3537-3548.
893 Jimenez, F., and Campos-Ortega, J.A. (1987). Genes in subdivision 1B of the *Drosophila*
894 *melanogaster* X-chromosome and their influence on neural development. Journal of
895 Neurogenetics *4*, 179-200.
896 Kale, A., Li, W., Lee, C.H., and Baker, N.E. (2015). Apoptotic mechanisms during competition
897 of ribosomal protein mutant cells: roles of the initiator caspases Dronc and Dream/Strica. Cell
898 Death Differ *22*, 1300-1312.
899 Kanuka, H., Kuranaga, E., Takemoto, K., Hiratou, T., Okano, H., and Miura, M. (2005).
900 Drosophila caspase transduces Shaggy/GSK-3beta kinase activity in neural precursor
901 development. EMBO J *24*, 3793-3806.
902 Kuranaga, E., and Miura, M. (2007). Nonapoptotic functions of caspases: caspases as regulatory
903 molecules for immunity and cell-fate determination. Trends Cell Biol *17*, 135-144.
904 Lee, J.D., and Treisman, J.E. (2002). Regulators of the morphogenetic furrow. Results Probl Cell
905 Differ *37*, 21-33.
906 Li, K., and Baker, N.E. (2018). Regulation of the Drosophila ID protein Extra macrochaetae by
907 proneural dimerization partners. Elife *7*, e33967.
908 Li, W., and Baker, N.E. (2007). Engulfment is required for cell competition. Cell *129*, 1215-
909 1225.
910 Li, Y., and Baker, N.E. (2001). Proneural enhancement by Notch overcomes Suppressor-of-
911 Hairless repressor function in the developing *Drosophila* eye. Current Biology *11*, 330-338.
912 Li, Y., and Baker, N.E. (2004). The roles of cis-inactivation by Notch ligands and of *neuralized*
913 during eye and bristle patterning in *Drosophila*. BioMed Central Developmental Biology *4*, 5.
914 Ling, F., Kang, B., and Sun, X.H. (2014). Id proteins: small molecules, mighty regulators. Curr
915 Top Dev Biol *110*, 189-216.
916 Little, J.C., Garcia-Garcia, E., Sul, A., and Kalderon, D. (2020). Drosophila hedgehog can act as
917 a morphogen in the absence of regulated Ci processing. Elife *9*.

Ma, C., and Moses, K. (1995). Wingless and patched are negative regulators of the morphogenetic furrow and can affect tissue polarity in the developing Drosophila compound eye. Development *121*, 2279-2289.

Ma, C., Zhou, Y., Beachy, P.A., and Moses, K. (1993). The segment polarity gene hedgehog is required for progression of the morphogenetic furrow in the developing Drosophila eye. Cell *75*, 927-938.

Massari, M.E., and Murre, C. (2000). Helix-loop-helix proteins: regulators of transcription in eucaryotic organisms. Mol Cell Biol *20*, 429-440.

Maurel-Zaffran, C., and Treisman, J.E. (2000). pannier acts upstream of wingless to direct dorsal eye disc development in Drosophila. Development *127*, 1007-1016.

Meier, P., Silke, J., Leevers, S.J., and Evan, G.I. (2000a). The *Drosophila* caspase DRONC is regulated by DIAP1. European Molecular Biology Organization Journal *19*, 598-611.

Meier, P., Silke, J., Leevers, S.J., and Evan, G.I. (2000b). The Drosophila caspase DRONC is regulated by DIAP1. EMBO J *19*, 598-611.

Micchelli, C.A., Rulifson, E.J., and Blair, S.S. (1997). The function and regulation of cut expression on the wing margin of Drosophila: Notch, Wingless and a dominant negative role for Delta and Serrate. Development *124*, 1485-1495.

Miller, A.C., Lyons, E.L., and Herman, T.G. (2009). cis-Inhibition of Notch by endogenous Delta biases the outcome of lateral inhibition. Curr Biol *19*, 1378-1383.

Motzny, C.K., and Holmgren, R. (1995). The *Drosophila* cubitus interruptus protein and its role in the *wingless* and *hedgehog* signal transduction pathways. Mechanisms of Development *52*, 137-150.

Nakajima, Y.I., and Kuranaga, E. (2017). Caspase-dependent non-apoptotic processes in development. Cell Death Differ *24*, 1422-1430.

Norton, J.D. (2000). ID helix-loop-helix proteins in cell growth, differentiation and tumorigenesis. J Cell Sci *113 (Pt 22)*, 3897-3905.

Ohlmeyer, J.T., and Kalderon, D. (1998). Hedgehog stimulates maturation of Cubitus interruptus into a labile transcriptional activator. Nature *396*, 749-753.

Oproescu, A.M., Han, S., and Schuurmans, C. (2021). New Insights Into the Intricacies of Proneural Gene Regulation in the Embryonic and Adult Cerebral Cortex. Front Mol Neurosci *14*, 642016.

Ou, C.Y., Lin, Y.F., Chen, D.F., and Chien, C.T. (2002). Distinct protein degradation mechanisms mediated by Cul1 and Cul3 controlling Ci stability in *Drosophila* eye development. Genes and Development *16*, 2403-2414.

Parks, A.L., Turner, R.F., and Muskavitch, M.A.T. (1995). Relationships between complex Delta expression and the specification of retinal fates during *Drosophila* eye development. Mechanisms of Development *50*, 201-216.

Pignoni, F., and Zipursky, L. (1997). Induction of *Drosophila* eye development by Decapentaplegic. Development *124*, 271-278.

Quinn, L.M., Dorstyn, L., Mills, K., Colussi, P.A., Chen, P., Coombe, M., Abrams, J., Kumar, S., and Richardson, H. (2000). An essential role for the caspase dronc in developmentally programmed cell death in Drosophila. J Biol Chem *275*, 40416-40424.

Reddy, V., Bhattacharya, A., and Baker, N.E. (2024). The Id protein Extramacrochaetae restrains the E-protein Daughterless to regulate Notch, Rap1, and Sevenless within the R7 equivalence group of the Drosophila eye Biology Open *in press*.

963 Roschger, C., and Cabrele, C. (2017). The Id-protein family in developmental and cancer-
964 associated pathways. Cell Commun Signal *15*, 7.
965 Sato, A., Kojima, T., Ui-Tei, K., Miyata, Y., and Saigo, K. (1999). Dfrizzled-3, a new
966 Drosophila Wnt receptor, acting as an attenuator of Wingless signaling in wingless hypomorphic
967 mutants. Development *126*, 4421-4430.
968 Shi, W., Stampas, A., Zapata, C., and Baker, N.E. (2003). The pineapple eye gene is required for
969 survival of Drosophila imaginal disc cells. Genetics *165*, 1869-1879.
970 Singh, S., Sarkar, T., Jakubison, B., Gadomski, S., Spradlin, A., Gudmundsson, K.O., and Keller,
971 J.R. (2022). Inhibitor of DNA binding proteins revealed as orchestrators of steady state, stress
972 and malignant hematopoiesis. Front Immunol *13*, 934624.
973 Spratford, C.M., and Kumar, J.P. (2013). Extramacrochaetae imposes order on the Drosophila
974 eye by refining the activity of the Hedgehog signaling gradient. Development *140*, 1994-2004.
975 Struhl, G., and Greenwald, I. (1999). Presenilin is required for activity and nuclear access of
976 Notch in Drosophila. Nature *398*, 522-525.
977 Su, T.T. (2020). Non-apoptotic roles of apoptotic proteases: new tricks for an old dog. Open Biol
978 *10*, 200130.
979 Tapadia, M.G., and Gautam, N.K. (2011). Non-apoptotic function of apoptotic proteins in the
980 development of Malpighian tubules of Drosophila melanogaster. J Biosci *36*, 531-544.
981 Tomlinson, A., and Struhl, G. (2001). Delta/Notch and Boss/Sevenless signals act
982 combinatorially to specify the *Drosophila* R7 photoreceptor. Molecular Cell *7*, 487-495.
983 Treisman, J.E. (2013). Retinal differentiation in Drosophila. Wiley Interdiscip Rev Dev Biol *2*,
984 545-557.
985 Treisman, J.E., and Rubin, G.M. (1995). wingless inhibits morphogenetic furrow movement in
986 the Drosophila eye disc. Development *121*, 3519-3527.
987 Verghese, S., Bedi, S., and Kango-Singh, M. (2012). Hippo signalling controls Dronc activity to
988 regulate organ size in Drosophila. Cell Death Differ *19*, 1664-1676.
989 Vrailas, A.D., and Moses, K. (2006). Smoothened, thickveins and the genetic control of cell
990 cycle and cell fate in the developing Drosophila eye. Mech Dev *123*, 151-165.
991 Wang, L.H., and Baker, N.E. (2015a). E Proteins and ID Proteins: Helix-Loop-Helix Partners in
992 Development and Disease. Dev Cell *35*, 269-280.
993 Wang, L.H., and Baker, N.E. (2015b). Salvador-Warts-Hippo pathway in a developmental
994 checkpoint monitoring helix-loop-helix proteins. Dev Cell *32*, 191-202.
995 Wang, L.H., and Baker, N.E. (2018). Spatial regulation of expanded transcription in the
996 Drosophila wing imaginal disc. PLoS One *13*, e0201317.
997 Wang, L.H., and Baker, N.E. (2019). Salvador-Warts-Hippo pathway regulates sensory organ
998 development via caspase-dependent nonapoptotic signaling. Cell Death Dis *10*, 669.
999 Wang, M., Zhao, X.M., Tan, H., Akutsu, T., Whisstock, J.C., and Song, J. (2014). Cascleave 2.0,
1000 a new approach for predicting caspase and granzyme cleavage targets. Bioinformatics *30*, 71-80.
1001 White, K., Grether, M.E., Abrams, J.M., Young, L., Farrell, K., and Steller, H. (1994). Genetic
1002 control of programmed cell death in Drosophila. Science *264*, 677-683.
1003 Xu, T., and Rubin, G.M. (1993). Analysis of genetic mosaics in developing and adult Drosophila
1004 tissues. Development *117*, 1223-1237.
1005 Xue, D., and Horvitz, H.R. (1995). Inhibition of the *Caenorhabditis elegans* cell-death protease
1006 CED-3 by a CED-3 cleavage site in baculovirus p35 protein. Nature *377*, 248-251.
1007 Ye, Y., Lukinova, N., and Fortini, M.E. (1999). Neurogenic phenotypes and altered Notch
1008 processing in Drosophila Presenilin mutants. Nature *398*, 525-529.

1009 Yoo, S.J., Huh, J.R., Muro, I., Yu, H., Wang, L., Wang, S.L., Feldman, R.M., Clem, R.J., Muller,
1010 H.A., and Hay, B.A. (2002). Hid, Rpr, and Grim negatively regulate DIAP1 levels through
1011 distinct mechanisms. Nature Cell Biology *4*, 416-424.
1012 Zeng, W., Wharton, K.A., Mack, J.A., Wang, K., Gadbaw, M., Suyama, K., Klein, P.S., and
1013 Scott, M.P. (2000). *naked cuticle* encodes an inducible antagonist of Wnt signalling. Nature *403*,
1014 789-795.
1015